2015

Impacts of various boundary conditions on beam vibrations

Ye Tao

IMPACTS OF VARIOUS BOUNDARY CONDITIONS ON BEAM VIBRATIONS

Ye Tao

Thesis submitted to the
Benjamin M. Statler College of Engineering and Mineral Resources
at West Virginia University
in partial fulfillment of the requirements for the degree of

Master of Science
in
Civil Engineering

Roger H. L. Chen, Ph.D., Chair
Omar Abdul-Aziz, Ph.D.
Horng-Jyh Yang, Ph.D.
Marvin Cheng., Ph.D.

Department of Civil Engineering and Environmental Engineering

Morgantown, West Virginia 2015
Keywords: Euler-Bernoulli Beam, Timoshenko Beam, Various Boundary Conditions, Free Vibrations, Forced Vibrations, Spring Constraints.

ABSTRACT

Impacts of Various Boundary Conditions on Beam Vibrations

Ye Tao

In real life, boundary conditions of most structural members are neither totally fixed nor completely free. It is crucial to study the effect of boundary conditions on beam vibrations. This thesis focuses on deriving analytical solutions to natural frequencies and mode shapes for Euler-Bernoulli Beams and Timoshenko Beams with various boundary conditions under free vibrations. In addition, Green's function method is employed to solve the close-form expression of deflection curves for forced vibrations of Euler-Bernoulli Beams and Timoshenko Beams.

A direct and general beam model is set up with two different vertical spring constraints k_{T1}, k_{T2} and two different rotational spring constraints k_{R1}, k_{R2} attached at the ends of the beam. These end constraints can represent various combinations of boundary conditions of the beam by varying the spring constraints. A general solution for the Timoshenko beam with this various boundary conditions is derived, and to the best of our knowledge, this solution is not available in the literature. Numerical examples are presented to illustrate the effects of the end constraints on the natural frequencies and mode shapes between Euler-Bernoulli beams and Timoshenko beam. The results show that Euler-Bernoulli beams have higher natural frequencies than Timoshenko beams at different modes. The ratio of the natural frequencies for Timoshenko beams to the natural frequency for Euler-Bernoulli beams decreases at higher modes. Natural frequencies at lower modes are more sensitive to boundary constraints than natural frequencies at higher modes.

ACKNOWLEGEMENTS

I would like to express my gratitude and appreciation to everyone who helped to make this thesis possible.

First of all, I would like to recognize my advisor Dr. Roger Chen for his superb guidance, incredible knowledge, proficient editing skills, and great support throughout my study at West Virginia University.

Second, I would like to thank my labmates Mr. Yun Lin, Mr. Zhanxiao Ma, and Mr. Alper Yikici for their assistance and suggestions during my project.

My thanks also go to other three committee members, Dr. Omar Abdul-Aziz, Dr. Hong-Jyh Yang, and Dr. Marvin Cheng for their advice, feedback, and direction. I would like to extend my appreciation to all the faculty and staff in the Department of Civil and Environmental Engineering at WVU.

Finally, I would like to thank my parents, Mrs. Hong Chen and Mr. Shijun Tao for their unconditioned love, constant encouragement, and extraordinary patience. I also feel blessed to have Di Wang accompany me in my life.

TABLE OF CONTENTS

LIST OF FIGURES

LIST OF TABLES

NOMENCLATURE

The following symbols are used in the thesis:

A = cross section area
E = Young's Modulus
G = modulus of rigidity
I = moment of inertia
k = dimensionless frequency of Euler-Bernoulli beams
K = numerical shape factor
k_{R1} = rotational spring constant on left hand side of the beam
k_{R2} = rotational spring constant on right hand side of the beam
k_{T1} = vertical spring constant on left hand side of the beam
k_{T2} = vertical spring constant on right hand side of the beam
$k\wedge$ = rotational spring constant $= \frac{k_{R1}L}{EI}$
L = beam length
M = bending moment
q = external load
t = time
V = shear force
Y = transverse deflection of the free vibration
ξ = dimensionless length = x/L
ξ_f = the point where the point load is applied at
Ψ = bending slope
ρ = density
ω = angular natural frequency of beam vibrations
ω_ω = angular frequency of the applied load
υ = Poisson ratio
b^2 = dimensionless frequency for Timoshenko beams = $\rho AL^4\omega^2 \,/\, (EI)$
r^2 = $I/(AL^2)$
s^2 = $EI/(KAGL^2)$

$$\alpha = \sqrt{\frac{1}{2}\left[-(r^2+s^2) + \sqrt{(r^2-s^2)^2+\frac{4}{b^2}}\right]}$$

$$\beta = \sqrt{\frac{1}{2}\left[(r^2+s^2) + \sqrt{(r^2-s^2)^2+\frac{4}{b^2}}\right]}$$

γ^4 = $\frac{\rho A L^4 \omega^2}{EI}$

f_T/f_{EB} = Natural frequency ratio of the Timoshenko beam to the Euler-Bernoulli beam

μ = $\sqrt{\frac{1}{2}[(r^2+s^2) - \sqrt{(r^2 - s^2)^2 + \frac{4}{b^2}}]}$

CHAPTER 1 Introduction

1.1 Introduction

Beam vibration is an important and interesting topic. Structures subjected to random vibrations can cause fatigue failures. When a beam is excited by a steady-state harmonic load, it vibrates at the same frequency as the frequency of the applied harmonic load. When the applied loading frequency equals to one of the natural frequencies of the system, large oscillation occurs, which can cause large beam deflection. This phenomenon is called resonance. Therefore, determination of natural frequencies is crucial in vibration problems.

Continuous structural beam systems are widely used in many engineering fields, such as structural engineering, transportation engineering, mechanical engineering, and aerospace engineering. The boundary conditions of structural members in continuous structural beam systems are indeterminate and complicated. It is not accurate to assume these boundary conditions as totally fixed or completely free.

In this thesis, a direct and general beam model is set up with two different rotational springs and two different vertical springs at both ends to simulate different beam boundary conditions. Dynamic responses of Euler-Bernoulli beams and Timoshenko beams under free vibrations and forced vibrations are analyzed. Euler-Bernoulli beam theory is also known as the classical beam theory. It is a simplification of the linear theory of elasticity which presents the relationship between the applied

load and the deflection of a slender beam. However the classical one-dimensional Euler-Bernoulli theory is not accurate enough for deep beams and the vibrations at higher modes. Timoshenko Beam theory counts in the effects of rotatory inertia and transverse-shear deformation, which are introduced by Rayleigh in 1842 and by Timoshenko in 1921, respectively. To the best of our knowledge, no one has derived the general solution for the Timoshenko beam vibration with arbitrary beam boundary conditions yet.

1.2 Objectives

The objectives of this thesis are: First, derive the solutions to the natural frequencies and the mode shapes of Euler-Bernoulli beams and Timoshenko beams with various boundary conditions under free vibration using eigenvalues and eigenvectors. Second, obtain the close-form expression of deflection shapes of Euler-Bernoulli beams and Timoshenko beams under forced vibrations using Green's function. Last, compare the effects of various boundary conditions on vibrations of Euler-Bernoulli beams and Timoshenko beams.

CHAPTER 2 Literature Review

2.1 Previous Studies

Vibrations of Euler-Bernoulli beams and Timoshenko beams have been studied by many researchers over the past decades. Huang (1961) presented normal modes and natural frequency equations of six types of Timoshenko beams with different end constraints under free vibrations: supported-supported beam, free-free beam, clamped-clamped beam, clamped-free beam, clamped-supported beam, and supported-free beam. Ross and Wang (1985) derived the frequency equation for a Timoshenko beam with two identical spring constraints k_R and two fixed vertical supports. Chen and Kiriakidis (2005) derived the frequency equation for the cantilever Timoshenko beam with a rotational spring and a vertical spring. Majkut (2009) analyzed the Timoshenko beam with identical vertical spring constraints k_T, and identical rotational spring constraints k_R at both ends. But he made a mistake on the equation of moments acting on infinitesimal beam element. The moment should be caused by pure bending angle, instead of the sum of bending angle and shear angle.

Different approaches have been employed to solve forced vibrations of Euler-Bernoulli beams and Timoshenko beams, such as the mode superposition method, and the dynamic Green's function method. Mode superposition method is an approximate method since truncations are used in the computation of the finite series. Hamada (1981) solved the solution for a simply supported and damped Euler-Bernoulli beam under a

moving load using double Laplace transform. Mackertich (1992) studied beam deflections of a simple supported Euler-Bernoulli beam and a simple supported Timoshenko beam using mode superposition method. Esmailzadeh and Ghorashi (1997) analyzed the dynamic response of a simply supported Timoshenko beam excited by uniformly distributed moving masses using finite difference method. Ekwaro-Osire et al. (2001) solved the deflection curve for a hinged-hinged Timoshenko beam by series expansion method. Uzzal et al. (2012) studied the vibrations of an Euler-Bernoulli beam supported on Pasternak foundation under a moving load by Fourier transform and mode superposition method. Azam et al. (2013) presented the dynamic response of a Timoshenko beam excited by a moving sprung mass using mode superposition method. Roshandel et al. (2015) investigated the dynamic response of a Timoshenko beam excited by a moving mass using Eigenfunction expansion method.

Green's function method is more straightforward and efficient compared to mode superposition method. There is no need to calculate natural frequencies and mode shapes for the beam for Green's function method. Many people have contributed to finding the corresponding Green's functions for beam vibrations. Mohamad (1994) tabulated the solutions for mode shapes of Euler-Bernoulli beams with intermediate attachments using Green's function. Lueschen (1996) derived the corresponding Green's function for forced Timoshenko beams vibrations in frequency domain using Laplace Transform for the same six beam types of as Huang's (1961). Foda and Abduljabbar (1997) studied the dynamic response of a simply supported Euler-Bernoulli beam under a moving mass using Green's function. Abu-Hilal (2003)

investigated the dynamic response of a cantilever Euler-Bernoulli beam with elastic support under distributed and concentrated loads using Green's function. Mehri et al. (2009) studied the forced vibrations of an Euler-Bernoulli beam with two identical rotational springs and two identical verticals springs under a moving load. Li and Zhao (2014) derived the steady-state Green's functions for deflection curve of forced vibrations of Timoshenko beam with a harmonic force considering damping effects for six types of beams for the same six beam types of as Huang's (1961).

However, to the best of our knowledge, the general solution to dynamic responses of a Timoshenko beam that can be applied to any arbitrary boundary conditions is not available in the literature yet.

2.2 Euler-Bernoulli Theory

Euler-Bernoulli theory is applied to a beam with one dimension much larger than the other two dimensions. There are three assumptions for the Euler-Bernoulli beam theory: First, the cross section is assumed to be elastic isotropic with small deflection. Second, the cross section of the beam remains plane after bending. Third, the cross section remains normal to the deformed axis of the beam.

The classical beam theory describes the relationship between the deflection of the beam, *y(x, t)* and the bending moment, $M(x,t)$:

$$M(x,t) = EI\frac{\partial^2 y}{\partial x^2} \tag{2.1}$$

y represents the transverse displacement of an element of the beam. *x* stands for the distance from the left hand end. *E* denotes the Young's modulus. *I(x)* is the moment of inertia of the section.

From Timoshenko's (1990) book *Vibration Problems in Engineering*, the mode shape for the Euler-Bernoulli beam under free vibration can be stated as:

$$y(x,t) = Y(x)T(t) \tag{2.2a}$$

$$Y(x) = C_1 sin(kx) + C_2 cos(kx) + C_3 sinh(kx) + C_4 cosh(kx) \tag{2.2b}$$

$$T(t) = Acos(\omega t) + Bsin(\omega t) \tag{2.2c}$$

k denotes the dimensionless frequency of the beam. ω denotes the angular frequency. C_1 to C_4 can be determined by the boundary conditions.

k and ω can be related to each other by:

$$\omega_i = (k_i)^2 \sqrt{\frac{EI}{\rho A}} \quad (i = 1, 2, 3, 4, 5 \ldots \ldots, \infty) \tag{2.3}$$

2.3 Timoshenko Beams Theory

Stephen Timoshenko introduced Timoshenko Beam theory in early 20th century (Timoshenko, 1921). The Timoshenko Beam theory takes effects of rotary inertia and shear deformations into account. It is suitable for describing the behavior of short beams, beams vibrating at high frequency modes. The extra mechanism of deformation reduces the stiffness of the beam, causing larger deflection and lower Eigen frequencies. The

governing equations of Timoshenko beams are 4^{th}order partial differential equations. The governing equations for Timoshenko Beams are shown as

$$EI\frac{\partial^2\varphi}{\partial x^2} + KAG\left(\frac{\partial y}{\partial x} - \varphi\right) - \rho I\frac{\partial^2\varphi}{\partial t^2} = 0 \tag{2.4a}$$

$$-\rho A\frac{\partial^2 y}{\partial t^2} + KAG\left(\frac{\partial^2 y}{\partial x^2} - \frac{\partial\varphi}{\partial x}\right) = 0 \tag{2.4b}$$

G, denotes modulus of rigidity; *A*, denotes cross section area; *K*, denotes numerical shape factor; *y*, denotes transverse deflection; φ denotes bending slope.

2.4 Green's Function

The concept of Green's function is developed by George Green in 1830s (Challis and Sheard 2003). Green's function is defined as the impulse response of a nonhomogeneous differential equation in a bounded region. It can be used to solve the solution to nonhomogeneous boundary value problems. It provides a visual interpretation of the response of a system with a unit point source.

Define a linear differential operator $\mathcal{L}$, acting on distributions over a subset of R^n Euclidean space. At a point x_f, a Green's function $G(x,x_f)$ has the following property:

$$\mathcal{L}\{G(x, x_f)\} = \delta\,(x - x_f) \tag{2.5}$$

δ is the Dirac delta function. The definition for Dirac delta function is:

$$\delta\,(x) = \begin{cases} +\infty & x = 0 \\ 0 & x \neq 0 \end{cases} \tag{2.6}$$

The Dirac delta function has an important property that

$$\int_{-\infty}^{\infty} f(x)\delta\,(x-a)\,dx = f(a) \tag{2.7}$$

Chapter 3 Free Vibrations of Euler-Bernoulli Beams

3.1 Natural Frequencies and Mode Shapes of an Euler-Bernoulli Beam with various boundary conditions

In real world, boundary conditions of a beam are complicated. In most cases, it is neither perfectly fixed, nor completely free. In this section, a general model of an Euler-Bernoulli beam is studied, which is a beam with two different rotational springs and two different vertical springs at the ends. It is demonstrated below:

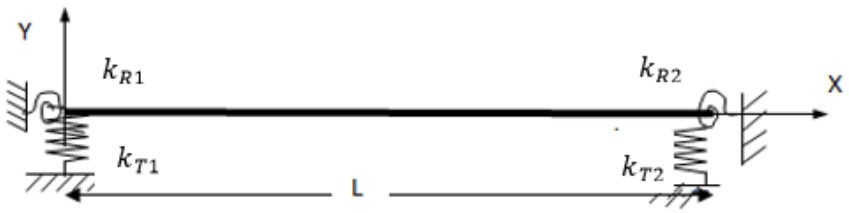

Figure 3.1: An Euler-Bernoulli Beam with Two Rotational Springs and Two Vertical Springs

k_{R1} and k_{T1} represent the rotational spring constant and the vertical spring on the left hand side of the beam, respectively. k_{R2} and k_{T2} represent the rotational spring constant and the vertical spring on the right hand side of the beam, respectively. By varying the spring constants of the two rotational springs and two vertical springs, various beam boundary conditions can be simulated.

The transverse vibration mode shape can be written as:

$$Y(\xi) = C_1 sin(k\xi) + C_2 cos(k\xi) + C_3 sinh(k\xi) + C_4 cosh(k\xi) \qquad (3.1)$$

where ξ is the dimensionless length x/L.

The boundary conditions are shown below:

$$M\big|_{\xi=0} = k_{R1}\Psi\big|_{\xi=0}, \quad M\big|_{\xi=1} = -k_{R2}\Psi\big|_{\xi=1}$$

$$V\big|_{\xi=0} = -k_{T1}Y\big|_{\xi=0}, \quad V\big|_{\xi=1} = k_{T2}Y\big|_{\xi=1} \tag{3.2}$$

Sign conventions for positive moment and positive shear are defined as:

Figure 3.2: Sign Convention

The bending moment *M*, bending slope Ψ, and shear force *V* can be calculated by:

$$M(\xi) = \frac{EIk^2}{L^2}[-C_1 sin(k\xi) - C_2 cos(k\xi) + C_3 sinh(k\xi) + C_4 cosh(k\xi)]$$

$$\Psi(\xi) = \frac{k}{L}[C_1 cos(k\xi) - C_2 sin(k\xi) + C_3 cosh(k\xi) + C_4 sinh(k\xi)]$$

$$V(\xi) = \frac{EIk^3}{L^3}[-C_1 cos(k\xi) + C_2 sin(k\xi) + C_3 cosh(k\xi) + C_4 sinh(k\xi)] \tag{3.3}$$

The boundary conditions can be rewritten in matrix format as:

$$\begin{bmatrix} k_{R1} & \frac{kEI}{L} & k_{R1} & -\frac{kEI}{L} \\ -\frac{EIk^3}{L^3} & k_{T1} & \frac{EIk^3}{L^3} & k_{T1} \\ -\frac{EIk^2}{L^2} sin(k) + \frac{k}{L} k_{R2} cos(k) & -\frac{EIk^2}{L^2} cos(k) - \frac{k}{L} k_{R2} sin(k) & \frac{EIk^2}{L^2} sinh(k) + \frac{k}{L} k_{R2} cosh(k) & \frac{EIk^2}{L^2} cosh\,(k) + \frac{k}{L} k_{R2} sinh(k) \\ -\frac{EIk^3}{L^3} cos(k) - k_{T2} sin(k) & \frac{EIk^3}{L^3} sin(k) - k_{T2} cos(k) & \frac{EIk^3}{L^3} cosh(k) - k_{T2} sinh(k) & \frac{EIk^3}{L^3} sinh(k) - k_{T2} cosh(k) \end{bmatrix} \times \begin{bmatrix} C_1 \\ C_2 \\ C_3 \\ C_4 \end{bmatrix} = \begin{bmatrix} 0 \\ 0 \\ 0 \\ 0 \end{bmatrix} \tag{3.4}$$

To find the nontrivial solution of C_1 to C_4, determinant of the four by four matrix must equal to zero. The frequency equation can be written as:

$$\left[-\frac{EIk^2}{L^2}sin(k)+\frac{k}{L}k_{R2}cos(k)\right]\times[\frac{kEI}{L}\times\frac{EIk^3}{L^3}\times\left(\frac{EIk^3}{L^3}sinh(k)-k_{T2}cosh(k)\right)+\ k_{R1}\times\ k_{T1}\times\left(\frac{EIk^3}{L^3}sin(k)-k_{T2}cos(k)\right)-\frac{kEI}{L}\times$$
$$k_{T1}\times\left(\frac{EIk^3}{L^3}cosh(k)-k_{T2}sinh(k)\right)+\frac{kEI}{L}\times\frac{EIk^3}{L^3}\times\left(\frac{EIk^3}{L^3}sin(k)-k_{T2}cos(k)\right)-\frac{kEI}{L}\times\ k_{T1}\left(\frac{EIk^3}{L^3}cosh(k)-k_{T2}\ sinh(k)\right)-\ k_{T1}\times\ k_{R1}\times$$
$$\left(\frac{EIk^3}{L^3}sinh(k)-k_{T2}cosh(k)\right)+\left[\frac{EIk^2}{L^2}cos(k)+\frac{k}{L}k_{R2}sin(k)\right]\times\left[k_{R1}\times\frac{EIk^3}{L^3}\left(\frac{EIk^3}{L^3}sinh(k)-k_{T2}cosh(k)\right)+\ k_{T1}\times\ k_{R1}\times\left(-\frac{EIk^3}{L^3}cos(k)-\right.\right.$$
$$k_{T2}sin(k)\Big)+\frac{kEI}{L}\times\frac{EIk^3}{L^3}\times\left(\frac{EIk^3}{L^3}cosh(k)-k_{T2}sinh(k)\right)+\frac{kEI}{L}\times\frac{EIk^3}{L^3}\times\left(-\frac{EIk^3}{L^3}cos(k)-k_{T2}sin(k)\right)-\ k_{T1}\times\ k_{R1}\times\left(\frac{EIk^3}{L^3}cosh(k)-\right.$$
$$\left.k_{T2}sinh(k)\right)+k_{R1}\times\frac{EIk^3}{L^3}\times\left(\frac{EIk^3}{L^3}sinh(k)-k_{T2}cosh(k)\right)\Big]+\left[\frac{EIk^2}{L^2}\times sinh(k)+\frac{k}{L}\times k_{R2}\times cosh(k)\right]\times[\ k_{T1}\times\ k_{R1}\times\left(\frac{EIk^3}{L^3}sinh(k)-\right.$$
$$k_{T2}cosh(k)\Big)+\frac{kEI}{L}\times\ k_{T1}\left(-\frac{EIk^3}{L^3}cos(k)-k_{T2}sin(k)\right)+\frac{kEI}{L}\times\frac{EIk^3}{L^3}\times\left(\frac{EIk^3}{L^3}sin(k)-k_{T2}cos(k)\right)+\frac{kEI}{L}\times\ k_{T1}\left(-\frac{EIk^3}{L^3}cos(k)-\right.$$
$$k_{T2}sin(k)\Big)-\ k_{T1}\times\ k_{R1}\times\left(\frac{EIk^3}{L^3}sin(k)-k_{T2}cos(k)\right)-\left[\frac{EIk^3}{L^3}sinh(k)-k_{T2}cosh(k)\right]\times\left[\ k_{R1}\times\ k_{T1}\times\left(\frac{EIk^3}{L^3}cosh(k)-k_{T2}sinh(k)\right)+\right.$$
$$\frac{kEI}{L}\times\frac{EIk^3}{L^3}\times\left(-\frac{EIk^3}{L^3}cos(k)-k_{T2}sin(k)\right)+\ k_{R1}\times\left(-\frac{EIk^3}{L^3}\right)\times\left(\frac{EIk^3}{L^3}sin(k)-k_{T2}cos(k)\right)-2\ k_{T1}\times k_{R1}\times\left(-\frac{EIk^3}{L^3}cos(k)-k_{T2}\times\right.$$
$$\left.\left.sin(k)\right)+\frac{kEI}{L}\times\frac{EIk^3}{L^3}\times\left(\frac{EIk^3}{L^3}cosh(k)-k_{T2}sinh(k)\right)\right]=0 \tag{3.5}$$

Eq. (3.5) can be solved using the MATLAB file shown in Appendix I, by inputting the values of $k_{R1},\ k_{T1},\ k_{R2},\ k_{T2}$.

The angular frequency can be calculated by:

$$\omega_i=\ (k_i/L)^2\sqrt{\frac{EI}{\rho A}}\quad (i=1,2,3,4,5\ldots\ldots,\infty) \tag{3.6}$$

3.2 Natural Frequencies and Mode Shapes of a Cantilever Euler-Bernoulli Beam with a Rotational Spring and a Vertical Spring

The natural frequencies and mode shapes of a cantilever Euler-Bernoulli beam with a rotational spring and a vertical spring under free vibrations are derived in this section using Eigenvalues and Eigenvectors. Blow is the sketch for the beam:

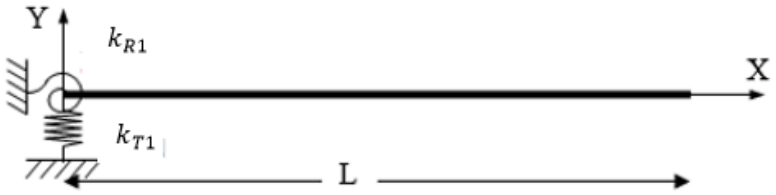

Figure 3.1: A Cantilever Euler-Bernoulli Beam with a Rotational Spring and a Vertical Spring

The boundary conditions are shown below:

$$M\big|_{\xi=0} = k_{R1}\Psi\big|_{\xi=0},\ M\big|_{\xi=1} = 0$$

$$V\big|_{\xi=0} = -k_{T1}Y\big|_{\xi=0},\ V\big|_{\xi=1} = 0 \qquad (3.7)$$

Plug in the equations of moment M, bending slope Ψ, shear V, and deflection Y into boundary conditions:

$$\begin{bmatrix} k_{R1} & \frac{kEI}{L} & k_{R1} & -\frac{kEI}{L} \\ -\frac{EIk^3}{L^3} & k_{T1} & \frac{EIk^3}{L^3} & k_{T1} \\ -\frac{EIk^2}{L^2}sin(k) & -\frac{EIk^2}{L^2}cos(k) & \frac{EIk^2}{L^2}sinh(k) & \frac{EIk^2}{L^2}cosh\,(k) \\ -\frac{EIk^3}{L^3}cos(k) & \frac{EIk^3}{L^3}sin(k) & \frac{EIk^3}{L^3}cosh(k) & \frac{EIk^3}{L^3}sinh(k) \end{bmatrix} \times \begin{bmatrix} C_1 \\ C_2 \\ C_3 \\ C_4 \end{bmatrix} = \begin{bmatrix} 0 \\ 0 \\ 0 \\ 0 \end{bmatrix}$$

(3.8)

In section 3.1, a general model of an Euler-Bernoulli beam has been studied with two different rotational springs and two different vertical springs at both ends. Assign zero to k_{T2} and k_{R2}, the general beam model is simplified to a cantilever Euler-Bernoulli beam with a rotational spring and a vertical spring, as shown in Figure 3.1. Eq. (3.4) can be reduced to:

$$\begin{bmatrix} k_{R1} & \frac{kEI}{L} & k_{R1} & -\frac{kEI}{L} \\ -\frac{EIk^3}{L^3} & k_{T1} & \frac{EIk^3}{L^3} & k_{T1} \\ -\frac{EIk^2}{L^2}sin(k) & -\frac{EIk^2}{L^2}cos(k) & \frac{EIk^2}{L^2}sinh(k) & \frac{EIk^2}{L^2}cosh\,(k) \\ -\frac{EIk^3}{L^3}cos(k) & \frac{EIk^3}{L^3}sin(k) & \frac{EIk^3}{L^3}cosh(k) & \frac{EIk^3}{L^3}sinh(k) \end{bmatrix} \times \begin{bmatrix} C_1 \\ C_2 \\ C_3 \\ C_4 \end{bmatrix} = \begin{bmatrix} 0 \\ 0 \\ 0 \\ 0 \end{bmatrix} \tag{3.9}$$

which is identical to Eq. (3.8) .

When k_{T1} and k_{R1} approach infinity, k_{T2} and k_{R2} equal to zero, the general beam becomes a cantilever beam. Below is the sketch:

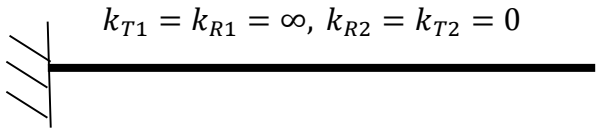

Figure 3.2: A cantilever Euler-Bernoulli Beam

Eq. (3.8) can be reduced to,

$$\begin{bmatrix} 1 & 0 & 1 & 0 \\ 0 & 1 & 0 & 1 \\ -\frac{EIk^2}{L^2}sin(k) & -\frac{EIk^2}{L^2}cos(k) & \frac{EIk^2}{L^2}sinh(k) & \frac{EIk^2}{L^2}cosh\,(k) \\ -\frac{EIk^3}{L^3}cos(k) & \frac{EIk^3}{L^3}sin(k) & \frac{EIk^3}{L^3}cosh(k) & \frac{EIk^3}{L^3}sinh(k) \end{bmatrix} \times \begin{bmatrix} C_1 \\ C_2 \\ C_3 \\ C_4 \end{bmatrix} = \begin{bmatrix} 0 \\ 0 \\ 0 \\ 0 \end{bmatrix} \tag{3.10}$$

by dividing the first row of Eq. (3.8) by k_{R1} and the second row of Eq. (3.8) by k_{T1}. The frequency equation can be simplified to:

$$cos(k) \times cosh(k) = -1 \tag{3.11}$$

Eq. (3.11) is identical with Timoshenko's (1990) result in the book of Vibration Problems in Engineering.

3.3 Natural Frequencies and Mode Shapes of an Euler-Bernoulli Beam with Two Rotational Springs and Two Fixed Vertical Supports

In this section, the free vibrations of an Euler-Bernoulli beam with two rotational springs and two fixed vertical supports are studied. The beam is plotted in Figure 3.3:

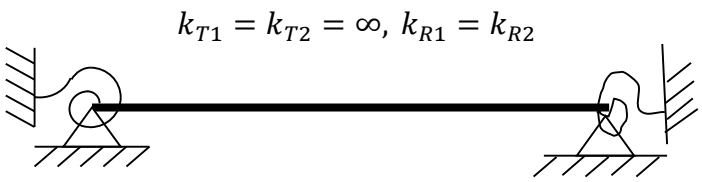

Figure 3.3: An Euler-Bernoulli Beam with Two Rotational Springs

The boundary conditions of the beam are:

$$M\big|_{\xi=0} = k_{R1}\Psi\big|_{\xi=0},\ M\big|_{\xi=1} = -k_{R1}\Psi\big|_{\xi=1}$$

$$Y\big|_{\xi=0} = 0,\ Y\big|_{\xi=1} = 0 \tag{3.12}$$

Substitute the equations of moment *M*, bending slope Ψ, and deflection *Y* into boundary conditions:

$$\begin{bmatrix} k_{R1} & \frac{kEI}{L} & k_{R1} & -\frac{kEI}{L} \\ 0 & 1 & 0 & 1 \\ -\frac{kEI}{L}sin(k) + k_{R1}cos(k) & -\frac{kEI}{L}cos(k) - k_{R1}sin(k) & \frac{kEI}{L}sinh(k) + k_{R1}cosh(k) & \frac{kEI}{L}cos(k) + k_{R1}sin(k) \\ sin(k) & cos(k) & sinh(k) & cosh(k) \end{bmatrix} \times \begin{bmatrix} C_1 \\ C_2 \\ C_3 \\ C_4 \end{bmatrix} = \begin{bmatrix} 0 \\ 0 \\ 0 \\ 0 \end{bmatrix}$$

(3.13)

Eq. (3.4) describes a set of four boundary conditions for a general beam model. Substitute k_{T1} and k_{T2} with infinity, k_{R2} with k_{R1}. Eq. (3.4) can be rewritten as:

$$\begin{bmatrix} k_{R1} & \frac{kEI}{L} & k_{R1} & -\frac{kEI}{L} \\ 0 & 1 & 0 & 1 \\ -\frac{kEI}{L}sin(k) + k_{R1}cos(k) & -\frac{kEI}{L}cos(k) - k_{R1}sin(k) & \frac{kEI}{L}sinh(k) + k_{R1}cosh(k) & \frac{kEI}{L}cos(k) + k_{R1}sin(k) \\ sin(k) & cos(k) & sinh(k) & cosh(k) \end{bmatrix} \times \begin{bmatrix} C_1 \\ C_2 \\ C_3 \\ C_4 \end{bmatrix} = \begin{bmatrix} 0 \\ 0 \\ 0 \\ 0 \end{bmatrix}$$

(3.14)

Eq. (3.14) matches Eq. (3.13) .

When k_{T1} and k_{T2} approach infinity, k_{R1} and k_{R2} go zero, the beam becomes a simply supported beam, as shown in Figure 3.4.

$$k_{T1} = k_{T2} = \infty,\ k_{R1} = k_{R2} = 0$$

Figure 3.4: A Simply Supported Euler-Bernoulli Beam

Eq. (3.13) can be reduced to:

$$\begin{bmatrix} 0 & \frac{kEI}{L} & 0 & -\frac{kEI}{L} \\ 0 & 1 & 0 & 1 \\ -\frac{kEI}{L}sin(k) & -\frac{kEI}{L}cos(k) & \frac{kEI}{L}sinh(k) & \frac{kEI}{L}cos(k) \\ sin(k) & cos(k) & sinh(k) & cosh(k) \end{bmatrix} \times \begin{bmatrix} C_1 \\ C_2 \\ C_3 \\ C_4 \end{bmatrix} = \begin{bmatrix} 0 \\ 0 \\ 0 \\ 0 \end{bmatrix} \tag{3.15}$$

The frequency equation can be simplified to:

$$sin(k) = 0 \tag{3.16}$$

Eq. (3.16) is verified with Timoshenko's (1990) results.

Chapter 4 Free Vibration of Timoshenko Beams

4.1 Timoshenko Beams under Free Vibrations

In chapter 3, free vibrations of Euler-Bernoulli beams have been studied. Euler-Bernoulli beam theory is accurate only for slender beams. Timoshenko beams theory takes into account of the shear deformation and the effects of rotary inertia. It is more accurate than Euler-Bernoulli beams for frequency calculations of deep beams, especially when beams are vibrating at higher mode.

The governing equations for Timoshenko Beams are given in *Vibration Problem in Engineering* (Timoshenko 1990):

$$EI\frac{\partial^2\varphi}{\partial x^2} + KAG\left(\frac{\partial y}{\partial x} - \varphi\right) - \rho I\frac{\partial^2\varphi}{\partial t^2} = 0 \tag{4.1}$$

$$-\rho A\frac{\partial^2 y}{\partial t^2} + KAG\left(\frac{\partial^2 y}{\partial x^2} - \frac{\partial\varphi}{\partial x}\right) = 0 \tag{4.2}$$

K is the numerical shape factor. y represents the lateral displacement. φ denotes the angle of rotation of the cross section due to bending.

Sign conventions for positive moment and positive shear are defined as:

Figure 4.1: Sign Convention for Timoshenko Beams

Moment and shear can be expressed as:

$$M(x,t) = EI\frac{\partial \varphi}{\partial x} \tag{4.3}$$

$$V(x,t) = -KAG\left(\frac{\partial y}{\partial x} - \varphi\right) \tag{4.4}$$

After applying of separation of variable methods (Huang 1961), Eqs. (4.1) and (4.2) can be stated as:

$$EI\frac{\partial^4 y}{\partial x^4} + \rho A\frac{\partial^2 y}{\partial t^2} - \left(\frac{EI\rho}{KG} + \rho I\right)\frac{\partial^4 y}{\partial x^2 \partial t^2} + \rho I\frac{\rho}{KG}\frac{\partial^4 y}{\partial t^4} = 0 \tag{4.5}$$

$$EI\frac{\partial^4 \varphi}{\partial x^4} + \rho A\frac{\partial^2 \varphi}{\partial t^2} - \left(\frac{EI\rho}{KG} + \rho I\right)\frac{\partial^4 \varphi}{\partial x^2 \partial t^2} + \rho I\frac{\rho}{KG}\frac{\partial^4 \varphi}{\partial t^4} = 0 \tag{4.6}$$

Transverse deflection *y*, and bending angle φ, can be written in term of dimensionless length ξ, and time *t*:

$$y = Y(\xi)\, e^{i\omega t} \tag{4.7}$$

$$\varphi = \Psi(\xi)\, e^{i\omega t} \tag{4.8}$$

Let's introduce three variables *b, r,* and *s*:

$$b^2 = \rho A L^4 \omega^2 / (EI) \tag{4.9}$$

$$r^2 = I/(AL^2) \tag{4.10}$$

$$s^2 = EI/(KAGL^2) \tag{4.11}$$

Substitute Eqs. (4.7) and (4.8) into Eqs. (4.5) and (4.6), then omit the $e^{i\omega t}$ on both sides of equations

$$Y^{IV} + b^2(r^2 + s^2)\, Y'' - b^2(1 - r^2 s^2 b^2)Y = 0 \tag{4.12}$$

$$\Psi^{IV} + b^2(r^2 + s^2)\, \Psi'' - b^2(1 - r^2 s^2 b^2)\Psi = 0 \tag{4.13}$$

Assume Y equals to $e^{\lambda\xi}$. Therefore, Eq. (4.12) becomes

$$\lambda^4 \times e^{\lambda\xi} + b^2(r^2 + s^2)\, e^{\lambda\xi} - b^2(1 - r^2 s^2 b^2)\, e^{\lambda\xi} = 0 \tag{4.14}$$

Eliminate $e^{\lambda\xi}$ on both sides. Eq. (4.14) can be reduced to:

$$\lambda^4 + \lambda^2 b^2(r^2 + s^2) - b^2(1 - r^2 s^2 b^2) = 0 \tag{4.15}$$

Let H equals to λ^2, then Eq. (4.15) can be written as

$$H^2 + b^2(r^2 + s^2)\, H - (1 - r^2 s^2 b^2) = 0 \tag{4.16}$$

Two roots of Eq. (4.16) are

$$H_1 = \frac{b^2}{2}\left[-(r^2 + s^2) + \sqrt{(r^2 - s^2)^2 + \frac{4}{b^2}}\,\right] \tag{4.17a}$$

$$H_2 = \frac{b^2}{2}\left[-(r^2 + s^2) - \sqrt{(r^2 - s^2)^2 + \frac{4}{b^2}}\right] \tag{4.17b}$$

When $\sqrt{(r^2 - s^2)^2 + \frac{4}{b^2}}$ is greater than $(r^2 + s^2)$, H_1 is positive. The four roots of Eq. (4.15) are

$$\lambda_1 = b\sqrt{\frac{1}{2}\left[-(r^2 + s^2) + \sqrt{(r^2 - s^2)^2 + \frac{4}{b^2}}\,\right]} \tag{4.18a}$$

$$\lambda_2 = -\,b\sqrt{\frac{1}{2}\left[-(r^2 + s^2) + \sqrt{(r^2 - s^2)^2 + \frac{4}{b^2}}\,\right]} \tag{4.18b}$$

$$\lambda_3 = i\,b\sqrt{\frac{1}{2}\left[(r^2 + s^2) + \sqrt{(r^2 - s^2)^2 + \frac{4}{b^2}}\,\right]} \tag{4.18c}$$

$$\lambda_4 = -i\, b \sqrt{\frac{1}{2}[\,(r^2 + s^2)\; + \sqrt{(r^2 - \; s^2)^2 + \frac{4}{b^2}}\,]} \tag{4.18d}$$

Let's define α and β:

$$\alpha = \sqrt{\frac{1}{2}[-(r^2 + s^2)\; + \; \sqrt{(r^2 - \; s^2)^2 + \frac{4}{b^2}}\,]} \tag{4.19}$$

$$\beta = \sqrt{\frac{1}{2}[(r^2 + s^2)\; + \; \sqrt{(r^2 - \; s^2)^2 + \frac{4}{b^2}}\,]} \tag{4.20}$$

Therefore, λ_1 to λ_4 can rewritten as

$$\lambda_1 = b\alpha,\; \lambda_2 = -b\alpha,\; \lambda_3 = b\beta i,\; \lambda_4 = -b\beta i \tag{4.21}$$

Y can be written as

$$Y(\xi) = C_1 e^{b\alpha\xi} + C_2\; e^{-b\alpha\xi} + C_3\; e^{b\beta\xi i} + C_4\; e^{-b\beta\xi i} \tag{4.22}$$

Eq. (4.22) can be rewritten as

$$Y\,(\xi) = C_1 \cosh(b\alpha\xi) + C_2\; sinh(b\alpha\xi)\; +\; C_3\; cos(b\beta\xi)\; + C_4\; sin(b\beta\xi) \tag{4.23}$$

Similarly, the bending angle can be Ψ derived. Ψ can be expressed as

$$\Psi(\xi) = D_1\; sinh\;(b\alpha\xi)\; + D_2\; cosh\;(b\alpha\xi)\; +\; D_3\; sin\;(b\beta\xi)\; + D_4\; cos\;(b\beta\xi) \tag{4.24}$$

Eq. (4.23) and Eq. (4.24) can be related to each other by the Eq. (4.6),

$$C_1 = \frac{L\alpha}{b(\alpha^2 + s^2)} D_1 \qquad\qquad C_2 = \frac{L\alpha}{b(\alpha^2 + s^2)} D_2$$

$$C_3 = -\frac{L\beta}{b(\beta^2 - s^2)} D_3 \qquad C_4 = \frac{L\beta}{b(\beta^2 - s^2)} D_4 \tag{4.25}$$

Deflection *Y* can be written as $Y(\xi) = \frac{L\alpha}{b(\alpha^2+s^2)} D_1 \cosh(b\alpha\xi) + \frac{L\alpha}{b(\alpha^2+s^2)} D_2 \sinh(b\alpha\xi) - \frac{L\beta}{b(\beta^2-s^2)} D_3 \cos(b\beta\xi) + \frac{L\beta}{b(\beta^2-s^2)} D_4 \sin(b\beta\xi)$ (4.26)

When $\sqrt{(r^2 - s^2)^2 + \frac{4}{b^2}}$ is less than $(r^2 + s^2)$, H_1 is a negative number. Following the same derivation procedure, *Y* and Ψ can be calculated as

$$Y(\xi) = C_1' \cos(b\mu\xi) + C_2' \sin(b\mu\xi) + C_3' \cos(b\beta\xi) + C_4' \sin(b\beta\xi) \tag{4.27}$$

$$\Psi(\xi) = D_1' \sin(b\mu\xi) + D_2' \cos(b\mu\xi) + D_3' \sin(b\beta\xi) + D_4' \cos(b\beta\xi) \tag{4.28}$$

where μ is $\sqrt{\frac{1}{2}[(r^2 + s^2) - \sqrt{(r^2 - s^2)^2 + \frac{4}{b^2}}\,]}$.

4.2 Natural Frequencies and Mode Shapes of a Timoshenko Beam with Various Boundary Conditions

In this chapter, a more general beam model is studied, which is a beam with two different rotational springs and two different verticals spring on ends. It has the ability to simulate all kinds of beam ends conditions. To the best of our knowledge, the frequencies and modes shapes of this beam model is not available in the literature. Below is the sketch of the beam:

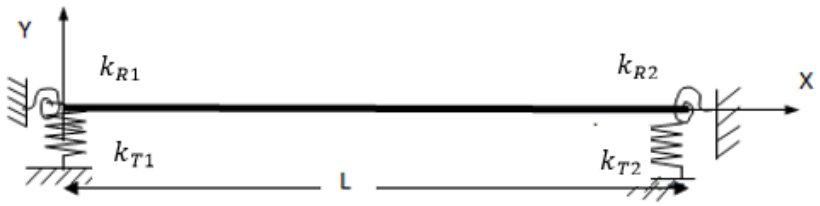

Figure 4.2: A Timoshenko Beam with Two Rotational Springs and Two Vertical Springs

Majkut (2009) discussed the frequencies and mode shapes of a Timoshenko beam with two identical vertical springs and two identical rotational springs at both ends, which is not as general as the beam studied in this section. However, he made a crucial mistake when he calculated the moment in page 199. The moment should be caused by pure bending angle alone, instead of both pure bending angle and shear angle.

The boundary conditions for this beam are

$$M\Big|_{\xi=0} = k_{R1}\Psi\Big|_{\xi=0} \quad V\Big|_{\xi=0} = -k_{T1}Y\Big|_{\xi=0}$$

$$M\Big|_{\xi=1} = -k_{R2}\Psi\Big|_{\xi=1} \quad V\Big|_{\xi=1} = k_{T2}Y\Big|_{\xi=1} \tag{4.29}$$

Deflection *Y*, bending angle Ψ, moment *M*, and shear force *V*, can be calculated as below

$$Y(\xi) = \frac{L\alpha}{b(\alpha^2+s^2)} D_1 \cosh(b\alpha\xi) + \frac{L\alpha}{b(\alpha^2+s^2)} D_2 \sinh(b\alpha\xi) - \frac{L\beta}{b(\beta^2-s^2)} D_3 \cos(b\beta\xi) + \frac{L\beta}{b(\beta^2-s^2)} D_4 sin(b\beta\xi) \quad (4.30)$$

$$\Psi(\xi) = D_1\, sinh(b\alpha\xi) + D_2\, cosh(b\alpha\xi) + D_3\, sin(b\beta\xi) + D_4\, cos(b\beta\xi) \quad (4.31)$$

$$M(\xi) = \frac{EIb\alpha}{L} cosh(b\alpha\xi) D_1 + \frac{EIb\alpha}{L} sinh(b\alpha\xi) D_2 + \frac{EIb\beta}{L} cos(b\beta\xi) D_3 - \frac{EIb\beta}{L} sin\,(b\beta\xi) D_4 \quad (4.32)$$

$$V(\xi) = KAG\,(\frac{s^2}{s^2+a^2} sinh\,(b\alpha\xi) D_1 + \frac{s^2}{s^2+a^2} cosh\,(b\alpha\xi) D_2 - \frac{s^2}{\beta^2-s^2} sin\,(b\beta\xi) D_3 - \frac{s^2}{\beta^2-s^2} cos\,(b\beta\xi) \quad (4.33)$$

Plug Eqs. (4.30) to (4.33) into boundary equations,

$$\begin{bmatrix} \frac{-k_{T1}L\alpha}{b(\alpha^2+s^2)} & \frac{-KAGs^2}{(\alpha^2+s^2)} & \frac{k_{T1}L\beta}{b(\beta^2-s^2)} & \frac{KAGs^2}{(\beta^2-s^2)} \\ \frac{EIb\alpha}{L} & -k_{R1} & \frac{EIb\beta}{L} & -k_{R1} \\ \frac{KAGs^2 b\,sinh(b\alpha) - k_{T2}L\alpha\cosh(b\alpha)}{b(\alpha^2+s^2)} & \frac{KAGs^2 bcosh(b\alpha) - k_{T2}L\alpha\sinh(b\alpha)}{b(\alpha^2+s^2)} & \frac{-KAGs^2 bsin(b\beta) + k_{T2}L\beta\cos(b\alpha)}{b(\beta^2-s^2)} & \frac{-KAGs^2 bcos(b\beta) - k_{T2}L\beta\sin(b\alpha)}{b(\beta^2-s^2)} \\ \frac{EIb\alpha\, cosh(b\alpha) + k_{R2}Lsinh(b\alpha)}{L} & \frac{EIb\alpha\, sinh(b\alpha) + k_{R2}Lcosh(b\alpha)}{L} & \frac{EIb\beta\, cos(b\alpha) + k_{R2}Lsin(b\alpha)}{L} & \frac{-EIb\beta\, sin(b\alpha) + k_{R2}Lcos(b\alpha)}{L} \end{bmatrix}$$

$$\times \begin{bmatrix} D_1 \\ D_2 \\ D_3 \\ D_4 \end{bmatrix} = \begin{bmatrix} 0 \\ 0 \\ 0 \\ 0 \end{bmatrix} \quad (4.34)$$

The frequency equation can be calculated by

$$\frac{-k_{T1}L\alpha}{b(\alpha^2+s^2)}\times\left[-k_{R1}\times\frac{-KAGs^2bsin(b\beta)+k_{T2}L\beta\,cos(b\alpha)}{b(\beta^2-s^2)}\times\frac{-EIb\beta\,sin(b\alpha)+k_{R2}Lcos(b\alpha)}{L}+\frac{-EIb\beta\,sin(b\alpha)+k_{R2}Lcos(b\alpha)}{L}\times\right.$$

$$\frac{-KAGs^2bcos(b\beta)-k_{T2}L\beta\,sin(b\alpha)}{b(\beta^2-s^2)}\times\frac{EIb\alpha\,sinh(b\alpha)+k_{R2}Lcosh(b\alpha)}{L}-k_{R1}\times\frac{KAGs^2bcosh(b\alpha)-k_{T2}L\alpha\,sinh(b\alpha)}{b(\alpha^2+s^2)}\times\frac{EIb\beta\,cos(b\alpha)+k_{R2}Lsin(b\alpha)}{L}+k_{R1}\times$$

$$\frac{-KAGs^2bsin(b\beta)+k_{T2}L\beta\,cos(b\alpha)}{b(\beta^2-s^2)}\times\frac{EIb\alpha\,sinh(b\alpha)+k_{R2}Lcosh(b\alpha)}{L}+k_{R1}\times\frac{-KAGs^2bcos(b\beta)-k_{T2}L\beta\,sin(b\alpha)}{b(\beta^2-s^2)}\times\frac{EIb\beta\,cos(b\alpha)+k_{R2}Lsin(b\alpha)}{L}-\frac{EIb\beta}{L}\times$$

$$\left.\frac{KAGs^2bcosh(b\alpha)-k_{T2}L\alpha\,sinh(b\alpha)}{b(\alpha^2+s^2)}\times\frac{-EIb\beta\,sin(b\alpha)+k_{R2}Lcos(b\alpha)}{L}\right]-\frac{-KAGs^2}{(\alpha^2+s^2)}\times\left[\frac{EIb\alpha}{L}\times\frac{-KAGs^2bsin(b\beta)+k_{T2}L\beta\,cos(b\alpha)}{b(\beta^2-s^2)}\times\right.$$

$$\frac{-EIb\beta\,sin(b\alpha)+k_{R2}Lcos(b\alpha)}{L}+\frac{EIb\beta}{L}\times\frac{-KAGs^2bcos(b\beta)-k_{T2}L\beta sin(b\alpha)}{b(\beta^2-s^2)}\times\frac{EIb\alpha\,cosh(b\alpha)+k_{R2}Lsinh(b\alpha)}{L}-k_{R1}\times$$

$$\frac{KAGs^2b\,sinh(b\alpha)-k_{T2}L\alpha cosh(b\alpha)}{b(\alpha^2+s^2)}\times\frac{EIb\beta\,cos(b\alpha)+k_{R2}Lsin(b\alpha)}{L}+k_{R1}\times\frac{-KAGs^2bsin(b\beta)+k_{T2}L\beta cos(b\alpha)}{b(\beta^2-s^2)}\times\frac{EIb\alpha\,cosh(b\alpha)+k_{R2}Lsinh(b\alpha)}{L}-$$

$$\left.\frac{EIb\alpha}{L}\times\frac{-KAGs^2bcos(b\beta)-k_{T2}L\beta sin(b\alpha)}{b(\beta^2-s^2)}\times\frac{EIb\beta\,cos(b\alpha)+k_{R2}Lsin(b\alpha)}{L}-\frac{EIb\beta}{L}\times\frac{KAGs^2b\,sinh(b\alpha)-k_{T2}L\alpha cosh(b\alpha)}{b(\alpha^2+s^2)}\times\frac{-EIb\beta\,sin(b\alpha)+k_{R2}Lcos(b\alpha)}{L}\right]+$$

$$\frac{k_{T1}L\beta}{b(\beta^2-s^2)}\times\left[\frac{EIb\alpha}{L}\times\frac{KAGs^2bcosh(b\alpha)-k_{T2}L\alpha sinh(b\alpha)}{b(\alpha^2+s^2)}\times\frac{-EIb\beta\,sin(b\alpha)+k_{R2}Lcos(b\alpha)}{L}-k_{R1}\times\frac{-KAGs^2bcos(b\beta)-k_{T2}L\beta\,sin(b\alpha)}{b(\beta^2-s^2)}\times\right.$$

$$\frac{EIb\alpha\,cosh(b\alpha)+k_{R2}Lsinh(b\alpha)}{L}-k_{R1}\times\frac{KAGs^2b\,sinh(b\alpha)-k_{T2}L\alpha cosh(b\alpha)}{b(\alpha^2+s^2)}\times\frac{EIb\alpha\,sinh(b\alpha)+k_{R2}Lcosh(b\alpha)}{L}+k_{R1}\times\frac{KAGs^2bcosh(b\alpha)-k_{T2}L\alpha sinh(b\alpha)}{b(\alpha^2+s^2)}\times$$

$$\frac{EIb\alpha\,cosh(b\alpha)+k_{R2}Lsinh(b\alpha)}{L}-\frac{EIb\alpha}{L}\times\frac{-KAGs^2bcos(b\beta)-k_{T2}L\beta sin(b\alpha)}{b(\beta^2-s^2)}\times\frac{EIb\alpha\,sinh(b\alpha)+k_{R2}Lcosh(b\alpha)}{L}+k_{R1}\times\frac{KAGs^2b\,sinh(b\alpha)-k_{T2}L\alpha cosh(b\alpha)}{b(\alpha^2+s^2)}\times$$

$$\left.\frac{-EIb\beta\,sin(b\alpha)+k_{R2}Lcos(b\alpha)}{L}\right]-\frac{KAGs^2}{(\beta^2-s^2)}\times\left[\frac{EIb\alpha}{L}\times\frac{KAGs^2bcosh(b\alpha)-k_{T2}L\alpha sinh(b\alpha)}{b(\alpha^2+s^2)}\times\frac{EIb\beta\,cos(b\alpha)+k_{R2}Lsin(b\alpha)}{L}-k_{R1}\times\right.$$

$$\frac{-KAGs^2 b\sin(b\beta)+k_{T_2}L\beta\cos(b\alpha)}{b(\beta^2-s^2)}\times\frac{EIb\alpha\cosh(b\alpha)+k_{R_2}L\sinh(b\alpha)}{L}+\frac{EIb\beta}{L}\times\frac{KAGs^2 b\sinh(b\alpha)-k_{T_2}L\alpha\cosh(b\alpha)}{b(\alpha^2+s^2)}\times\frac{EIb\alpha\sinh(b\alpha)+k_{R_2}L\cosh(b\alpha)}{L}-\frac{EIb\beta}{L}\times$$

$$\frac{KAGs^2 b\cosh(b\alpha)-k_{T_2}L\alpha\sinh(b\alpha)}{b(\alpha^2+s^2)}\times\frac{EIb\alpha\cosh(b\alpha)+k_{R_2}L\sinh(b\alpha)}{L}-\frac{EIb\alpha}{L}\times\frac{-KAGs^2 b\sin(b\beta)+k_{T_2}L\beta\cos(b\alpha)}{b(\beta^2-s^2)}\times\frac{EIb\alpha\sinh(b\alpha)+k_{R_2}L\cosh(b\alpha)}{L}+k_{R1}\times$$

$$\frac{KAGs^2 b\sinh(b\alpha)-k_{T_2}L\alpha\cosh(b\alpha)}{b(\alpha^2+s^2)}\times\frac{EIb\beta\cos(b\alpha)+k_{R_2}L\sin(b\alpha)}{L}]=0 \qquad (4.35)$$

Dimensionless frequency *b*, can be obtained by solving Eq. (4.35) using the MATLAB file in Appendix II.

The angular frequency can be calculated as by:

$$\omega_i = (b_i/L)^2\sqrt{\frac{EI}{\rho A}} \quad (\mathrm{i}=1,2,3,4,5\ldots\ldots,\infty) \qquad (4.36)$$

4.3 Natural Frequencies and Mode Shapes of a Cantilever Timoshenko Beam with a Rotational Spring and a Vertical Spring

In this section, the free vibration of a cantilever Timoshenko beam with a rotational spring and a vertical spring is analyzed. The beam is demonstrated below:

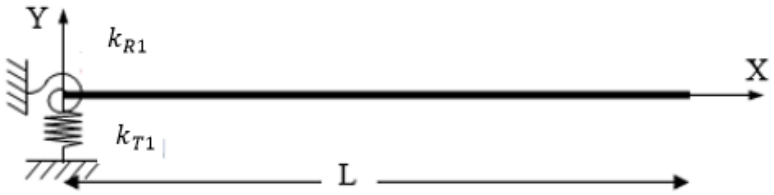

Figure 4.3: A Cantilever Timoshenko Beam with a Rotational Spring and a Vertical Spring

The boundary conditions are shown below:

$$M\big|_{\xi=0} = k_{R1}\Psi\big|_{\xi=0},\ M\big|_{\xi=1} = 0$$

$$V\big|_{\xi=0} = -k_{T1}Y\big|_{\xi=0},\ V\big|_{\xi=1} = 0 \tag{4.37}$$

Plug Eqs. (4.30) to (4.33) into boundary equations,

$$\begin{bmatrix} \frac{-k_{T1}L\alpha}{b(\alpha^2+s^2)} & \frac{-KAGs^2}{(\alpha^2+s^2)} & \frac{k_{T1}L\beta}{b(\beta^2-s^2)} & \frac{KAGs^2}{(\beta^2-s^2)} \\ \frac{EIb\alpha}{L} & -k_{R1} & \frac{EIb\beta}{L} & -k_{R1} \\ \frac{KAGs^2}{s^2+a^2}sinh\,(b\alpha) & \frac{KAGs^2}{s^2+a^2}cosh\,(b\alpha) & -\frac{KAGs^2}{\beta^2-s^2}\,sin\,(b\beta) & -\frac{KAGs^2}{\beta^2-s^2}\,cos\,(b\beta) \\ \frac{EIb\alpha}{L}cosh(b\alpha) & \frac{EIb\alpha}{L}\,sinh\,(b\alpha) & \frac{EIb\beta}{L}\,cos\,(b\beta) & -\frac{EIb\beta}{L}\,sin\,(b\beta) \end{bmatrix}$$

$$\times \begin{bmatrix} C_1 \\ C_2 \\ C_3 \\ C_4 \end{bmatrix} = \begin{bmatrix} 0 \\ 0 \\ 0 \\ 0 \end{bmatrix}$$

(4.38)

The boundary conditions of the general Timoshenko beam under free vibrations are described by a set of four homogenous equations in Eq. (4.34) . Let k_{T2} and k_{R2} equal to zero, the beam becomes to a cantilever beam with a rotational spring and a vertical spring, as shown in Figure 4.3. Eq. (4.34) can be simplified to be:

$$\begin{bmatrix} \frac{-k_{T1}L\alpha}{b(\alpha^2+s^2)} & \frac{-KAGs^2}{(\alpha^2+s^2)} & \frac{k_{T1}L\beta}{b(\beta^2-s^2)} & \frac{KAGs^2}{(\beta^2-s^2)} \\ \frac{EIb\alpha}{L} & -k_{R1} & \frac{EIb\beta}{L} & -k_{R1} \\ \frac{KAGs^2}{s^2+a^2}sinh\,(b\alpha) & \frac{KAGs^2}{s^2+a^2}cosh\,(b\alpha) & -\frac{KAGs^2}{\beta^2-s^2}\,sin\,(b\beta) & -\frac{KAGs^2}{\beta^2-s^2}\,cos\,(b\beta) \\ \frac{EIb\alpha}{L}cosh(b\alpha) & \frac{EIb\alpha}{L}\,sinh\,(b\alpha) & \frac{EIb\beta}{L}\,cos\,(b\beta) & -\frac{EIb\beta}{L}\,sin\,(b\beta) \end{bmatrix}$$

$$\times \begin{bmatrix} C_1 \\ C_2 \\ C_3 \\ C_4 \end{bmatrix} = \begin{bmatrix} 0 \\ 0 \\ 0 \\ 0 \end{bmatrix} \qquad (4.39)$$

Eq. (4.39) is identical to Eq. (4.38) .

The frequency equation of the cantilever beam with a rotational spring and a vertical spring can be written as:

$$b^2EIKAGS^2\left[2-2\,cosh(b\alpha)\,cos(b\beta)+\frac{b[b^2r^2(r^2-s^2)+(3r^2-s^2)}{\sqrt{1-b^2r^2s^2}}sinh(b\alpha)\,sin(b\beta)\right]+$$

$$k_Rk_TL^2\left[2+(b^2(r^2-s^2)^2+2)\,cosh(b\alpha)\,cos(b\beta)-\frac{b(r^2+s^2)}{\sqrt{1-b^2r^2s^2}}sinh(ba)\,sin(b\beta)\right]+$$

$$k_TEILb^3(\alpha^2+\beta^2)[\alpha(\alpha^2+s^2)\,sinh(b\alpha)\,cos(b\beta)-\beta(\beta^2-s^2)\,cosh(b\alpha)\,sin(b\beta)-$$

$$k_RKAGLb^3s^2\frac{\alpha^2+\beta^2}{\alpha\beta}[\beta(\beta^2-s^2)\,sinh(b\alpha)\,cos(b\beta)+\alpha(\alpha^2+s^2)\,cosh(b\alpha)\,sin(b\beta)=0 \quad (4.40)$$

Eq. (4.40) can be validated with Chen and Kiriakidis's (2005) frequency equation.

Let k_{T1} and k_{R1} go to infinity, k_{T2} and k_{R2} equal to zero, the beam becomes a cantilever beam.

Eq. (4.38) can be reduced to be:

$$\begin{bmatrix} \frac{-L\alpha}{b(\alpha^2+s^2)} & 0 & \frac{L\beta}{b(\beta^2-s^2)} & 0 \\ 0 & -1 & 0 & -1 \\ \frac{KAGs^2}{s^2+a^2}sinh\,(b\alpha) & \frac{KAGs^2}{s^2+a^2}cosh\,(b\alpha) & -\frac{KAGs^2}{\beta^2-s^2}\,sin\,(b\beta) & -\frac{KAGs^2}{\beta^2-s^2}\,cos\,(b\beta) \\ \frac{EIb\alpha}{L}cosh(b\alpha) & \frac{EIb\alpha}{L}\,sinh\,(b\alpha) & \frac{EIb\beta}{L}\,cos\,(b\beta) & -\frac{EIb\beta}{L}\,sin\,(b\beta) \end{bmatrix}$$

$$\times \begin{bmatrix} C_1 \\ C_2 \\ C_3 \\ C_4 \end{bmatrix} = \begin{bmatrix} 0 \\ 0 \\ 0 \\ 0 \end{bmatrix} \quad (4.41)$$

The frequency of the cantilever beam can be calculated by

$$2 + [b^2 (r^2 - s^2)^2 + 2]cosh(b\alpha)cos(b\beta) - \frac{b (r^2 + s^2)}{(1 - r^2 s^2 b^2)} sinh(b\alpha)sin(b\beta) = 0 \quad (4.42)$$

Eq. (4.42) matches Huang's (1961) results.

4.4 Natural Frequencies and Mode Shapes of a Timoshenko Beam with Two Rotational Springs and Two Fixed Vertical Supports

The natural frequencies and mode shapes of a Timoshenko beam with two rotational spring and two fixed vertical supports are derived in this section. Blow is the sketch of the beam:

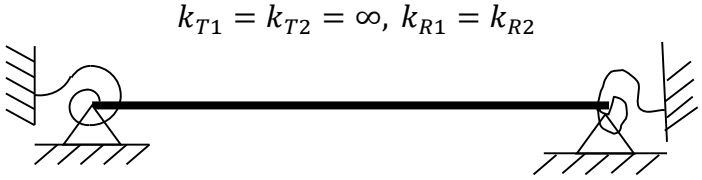

Figure 4.4: A Timoshenko Bernoulli Beam with Two Rotational Springs

The boundary conditions of the beam are:

$$M\big|_{\xi=0} = k_{R1}\Psi\big|_{\xi=0}$$

$$M\big|_{\xi=1} = -k_{R1}\Psi\big|_{\xi=1}$$

$$Y\big|_{\xi=0} = 0$$

$$Y\big|_{\xi=1} = 0 \quad (4.43)$$

Substitute Eqs. (4.30) to (4.33) into boundary equations,

$$\begin{bmatrix} \frac{L\alpha}{b(\alpha^2+s^2)} & 0 & -\frac{L\beta}{b_i(\beta^2-s^2)} & 0 \\ \frac{EIb\alpha}{L} & -k_{R1} & \frac{EIb\beta}{L} & -k_{R1} \\ \frac{L\alpha}{b(\alpha^2+s^2)}cosh(b\alpha) & \frac{L\alpha}{b(\alpha^2+s^2)}sinh(b\alpha) & -\frac{L\beta}{b(\beta^2-s^2)}cos(b\beta) & \frac{L\beta}{b(\beta^2-s^2)}sin(b\beta) \\ \frac{EIb\alpha\, cosh(b\alpha)+k_{R1}\, Lsinh(b\alpha)}{L} & \frac{EIb\alpha\, sinh(b\alpha)+k_{R1}\, Lcosh(b\alpha)}{L} & \frac{EIb\beta\, cos(b\alpha)+k_{R1}\, Lsin(b\alpha)}{L} & \frac{-EIb\beta\, sin(b\alpha)+k_{R1}\, Lcos(b\alpha)}{L} \end{bmatrix} \times \begin{bmatrix} D_1 \\ D_2 \\ D_3 \\ D_4 \end{bmatrix} = \begin{bmatrix} 0 \\ 0 \\ 0 \\ 0 \end{bmatrix}$$

(4.44)

Substitute k_{T1} and k_{T2} with infinity, k_{R2} with k_{R1} into Eq. (4.42) ,

$$\begin{bmatrix} \frac{L\alpha}{b(\alpha^2+s^2)} & 0 & -\frac{L\beta}{b_i(\beta^2-s^2)} & 0 \\ \frac{EIb\alpha}{L} & -k_{R1} & \frac{EIb\beta}{L} & -k_{R1} \\ \frac{L\alpha}{b(\alpha^2+s^2)}cosh(b\alpha) & \frac{L\alpha}{b(\alpha^2+s^2)}sinh(b\alpha) & -\frac{L\beta}{b(\beta^2-s^2)}cos(b\beta) & \frac{L\beta}{b(\beta^2-s^2)}sin(b\beta) \\ \frac{EIb\alpha\, cosh(b\alpha)+k_{R1}\, Lsinh(b\alpha)}{L} & \frac{EIb\alpha\, sinh(b\alpha)+k_{R1}\, Lcosh(b\alpha)}{L} & \frac{EIb\beta\, cos(b\alpha)+k_{R1}\, Lsin(b\alpha)}{L} & \frac{-EIb\beta\, sin(b\alpha)+k_{R1}\, Lcos(b\alpha)}{L} \end{bmatrix} \times \begin{bmatrix} D_1 \\ D_2 \\ D_3 \\ D_4 \end{bmatrix} = \begin{bmatrix} 0 \\ 0 \\ 0 \\ 0 \end{bmatrix}$$

(4.45)

Eq. (4.43) matches Eq. (4.44) .

The frequency equation of the beam can be written as:

$$\frac{L\alpha}{b(\alpha^2+s^2)}\times\left(k_{R1}\times\frac{L\beta}{b(\beta^2-s^2)}\cos(b\beta)\times\frac{-EIb\beta\,sin(b\alpha)+k_{R1}Lcos(b\alpha)}{L}+\frac{EIb\beta}{L}\times\frac{L\beta}{b(\beta^2-s^2)}\times sin\,(b\beta)\times\right.$$

$$\frac{EIb\alpha\,cosh(b\alpha)+k_{R1}Lsinh(b\alpha)}{L}+k_{R1}\times\frac{L\alpha}{b(\alpha^2+s^2)}sinh\,(b\alpha)\times\frac{EIb\beta\,cos(b\alpha)+k_{R1}Lsin(b\alpha)}{L}-k_{R1}\times\frac{L\beta}{b(\beta^2-s^2)}\,cos\,(b\beta)\times$$

$$\frac{EIb\alpha\,sinh(b\alpha)+k_{R1}Lcosh(b\alpha)}{L}-k_{R1}\times\frac{L\beta}{b(\beta^2-s^2)}\,sin\,(b\beta)\times\frac{EIb\beta\,cos(b\alpha)+k_{R1}Lsin(b\alpha)}{L}-\frac{EIb\beta}{L}\times\frac{L\alpha}{b(\alpha^2+s^2)}\,sinh\,(b\alpha)\times$$

$$\left.\frac{-EIb\beta\,sin(b\alpha)+k_{R1}Lcos(b\alpha)}{L}\right]-\frac{L\beta}{b(\beta^2-s^2)}\times\left[\frac{EIb\alpha}{L}\times\frac{L\alpha}{b(\alpha^2+s^2)}\sinh(b\alpha)\times\frac{-EIb\beta\,sin(b\alpha)+k_{R1}Lcos(b\alpha)}{L}+k_{R1}\times\sin(b\beta)\times\right.$$

$$\frac{EIb\alpha\,cosh(b\alpha)+k_{R1}Lsinh(b\alpha)}{L}-k_{R1}\,\frac{L\alpha}{b(\alpha^2+s^2)}\,\cosh(b\alpha)\times\frac{EIb\alpha\,sinh(b\alpha)+k_{R1}Lcosh(b\alpha)}{L}+k_{R1}\times$$

$$\frac{L\alpha}{b(\alpha^2+s^2)}\,sinh\,(b\alpha)\,\frac{EIb\alpha\,cosh(b\alpha)+k_{R1}Lsinh(b\alpha)}{L}-\frac{EIb\alpha}{L}\times\frac{L\beta}{b(\beta^2-s^2)}\,sin\,(b\beta)\times\frac{EIb\alpha\,sinh(b\alpha)+k_{R1}Lcosh(b\alpha)}{L}-k_{R1}\,\frac{L\alpha}{b(\alpha^2+s^2)}\times$$

$$cosh\,(b\alpha)\times\frac{-EIb\beta\,sin(b\alpha)+k_{R1}Lcos(b\alpha)}{L}=0 \qquad (4.46)$$

Eq. (4.45) can be converted to Ross's (1985) frequency equation by following his notations.

When k_{T1} and k_{T2} approach infinity, k_{R1} and k_{R2} go zero, the beam becomes a simply supported beam. Eq. (4.43) can be reduced to

$$\begin{bmatrix} \frac{L\alpha}{b(\alpha^2+s^2)} & 0 & -\frac{L\beta}{b(\beta^2-s^2)} & 0 \\ \frac{EIb\alpha}{L} & 0 & \frac{EIb\beta}{L} & 0 \\ \frac{L\alpha}{b(\alpha^2+s^2)}cosh(b\alpha) & \frac{L\alpha}{b(\alpha^2+s^2)}sinh(b\alpha) & -\frac{L\beta}{b(\beta^2-s^2)}cos(b\beta) & \frac{L\beta}{b(\beta^2-s^2)}\sin(b\beta) \\ \frac{EIb\alpha}{L}\cosh(b\alpha) & \frac{EIb\alpha}{L}\sinh(b\alpha) & \frac{EIb\beta}{L}\cos(b\beta) & -\frac{EIb\beta}{L}\sin(\mathrm{b}\beta) \end{bmatrix} \times \begin{bmatrix} D_1 \\ D_2 \\ D_3 \\ D_4 \end{bmatrix} = \begin{bmatrix} 0 \\ 0 \\ 0 \\ 0 \end{bmatrix} \quad (4.47)$$

The frequency of the simply supported beam can be stated as

$$sin\ (b\beta) = 0 \quad (4.48)$$

Eq. (4.47) is identical to Huang's (1961) results.

CHAPTER 5 Forced Vibrations of Euler-Bernoulli Beams

5.1 Deflection Curves of Forced Vibrations of Euler-Bernoulli Beams

In this section, the deflection curve of forced vibrations of Euler-Bernoulli beams with an arbitrary exciting distributed force $q(\xi,t)$ are presented. $q(\xi,t)$ points upwards. The governing equation for the Euler-Bernoulli beam is

$$\frac{EI}{L^4}\frac{\partial^4 y}{\partial \xi^4} + \rho A \frac{\partial^2 y}{\partial t^2} = q(\xi, t) \tag{5.1}$$

Apply Laplace transform to Eq. (5.1),

$$\frac{EI}{L^4} y^{IV}(\xi, \omega) - \rho A \omega^2 \, y(\xi, \omega) = \mathrm{q}(\xi, \omega) \tag{5.2}$$

The forced vibration shape of an Euler-Bernoulli beam can be written as a Green function in order for the beam to be in a steady state:

$$y(\xi, t) = G(\xi, \xi_f) \, exp(i\omega t) \tag{5.3}$$

where ξ_f is the point where the arbitrary force is applied at.

Eq. (5.2) can be rewritten as

$$\frac{EI}{L^4} G^{IV}\left(\xi, \xi_f\right) - \rho A \omega^2 \, G\left(\xi, \xi_f\right) = \delta(\xi - \xi_f) \tag{5.4}$$

In this section, the effects of internal damping and external damping are neglected. The vibration functions derived in this section are for dimensionless frequencies *b*, lower than cut-off frequency: $\sqrt{(r^2 - s^2)^2 + \frac{4}{b^2}} > (r^2 + s^2)$, which can be rewritten as $b < \frac{1}{r^2 s^2}$.

$G(\xi, \xi_f)$ is summation of two parts: homogenous solution, and particular solution.

$$G(\xi, \xi_f) = G_0(\xi) + G_1(\xi, \xi_f) H(\xi - \xi_f) \tag{5.5}$$

where $H(\xi - \xi_f)$ is the step function. It has the property that when ξ is smaller than ξ_f, the function equals to 0; when ξ is bigger than ξ_f, the function equals to 1.

$G_0(\xi)$ is the solution to homogeneous equation, which can be stated as:

$$G_0(\xi) = C_1 \sin(k\xi) + C_2 \cos(k\xi) + C_3 \sinh(k\xi) + C_4 \cosh(k\xi) \tag{5.6}$$

k is the dimensionless frequency, which can be written as:

$$k = \left(\frac{EI\omega^2 L^4}{\rho A}\right)^{1/4} \tag{5.7}$$

$G_1(\xi, \xi_f)$ is the solution to inhomogeneous equation, which can be written as:

$$G_1(\xi, \xi_f) = P_1 \cosh[k(\xi - \xi_f)] + P_2 \sinh[k(\xi - \xi_f)] + P_3 \cos[k(\xi - \xi_f)] + P_4 \sin[k(\xi - \xi_f)] \tag{5.8}$$

From continuity conditions

$$G(\xi_f^+, \xi_f) - G(\xi_f^-, \xi_f) = 0 \tag{5.9a}$$

$$\Psi(\xi_f^+, \xi_f) - \Psi(\xi_f^-, \xi_f) = 0 \tag{5.9b}$$

$$M(\xi_f{}^+,\ \xi_f) - M(\xi_f{}^-,\ \xi_f) = 0 \tag{5.9c}$$

$$V(\xi_f{}^+,\ \xi_f) - V(\xi_f{}^-,\ \xi_f) = 1 \tag{5.9d}$$

Bending slope Ψ, moment M, and shear force V, can be calculated by:

$$\Psi(\xi, \xi_f) = \frac{dG}{dx} = \frac{1}{L}\frac{dG}{d\xi} \tag{5.10}$$

$$M(\xi,\ \xi_f) = EI\ \frac{d^2G}{dx^2} = \frac{EI}{L^2}\frac{d^2G}{d\xi^2} \tag{5.11}$$

$$V(\xi, \xi_f) = EI\ \frac{d^3G}{dx^3} = \frac{EI}{L^3}\frac{d^3G}{d\xi^3} \tag{5.12}$$

Apply Eqs. (5.8), (5.10), (5.11), and (5.12), into continuity conditions. After simplification, we get the following terms

$$P_1 + P_3 = 0 \tag{5.13a}$$

$$\frac{k}{L}(P_2 + P_4) = 0 \tag{5.13b}$$

$$\frac{EIk^2}{L^2}(P_1 - P_3) = 0 \tag{5.13c}$$

$$\frac{EIk^3}{L^3}(P_2 - P_4) = 1 \tag{5.13d}$$

Therefore, the four terms can be solved, which are

$$P_1 = 0, P_2 = \frac{L^3}{2EIk^3},\ P_3 = 0,\ P_4 = -\frac{L^3}{2EIk^3} \tag{5.14}$$

The close-form expression of forced vibration shape can be written as

$$G(\xi,\xi_f) \;=\; C_1\sin(k\xi) + C_2\cos(k\xi) + C_3\sinh(k\xi) + C_4\cosh(k\xi) + \frac{L^3}{2EIk^3}\times$$

$$sinh\big[\,k\big(\xi\;-\;\xi_f\big)\big]H[k(\xi\;-\;\xi_f)] - \frac{L^3}{2EIk^3}sin[\,k(\xi\;-\;\xi_f))]\,H(k(\xi\;-\;\xi_f))]$$

(5.15)

5.2 Forced Vibrations of Euler-Bernoulli Beams with Two Different Rotational Springs and Two Different Vertical Springs

A highly simply and general beam model is set up with two different rotational springs and two vertical springs at both ends. The sketch has been presented Figure 3.1. To the best of my knowledge, the force vibration of the general Timoshenko beam has not been studied by others yet.

The deflection G, bending slope φ, moment M, and shear V can be written as

$$G(\xi,\xi_f) \;=\; C_1\sin(k\xi) + C_2\cos(k\xi) + C_3\sinh(k\xi) + C_4\cosh(k\xi) + \frac{L^3}{2EIk^3}\times$$

$$[\,k(\xi\;-\xi_f)]\,H(\xi-\xi_f)] - \frac{L^3}{2EIk^3}sin[\,k(\xi\;-\xi_f)]\,H(\xi-\xi_f)]$$

(5.16)

$$\Psi\,(\xi,\xi_f) \;=\; \frac{k}{L}\,\big[C_1\,cos(k\xi) - C_2\,sin(k\xi) + C_3\,cosh(k\xi) + C_4\,sinh(k\xi) + \frac{L^3}{2EIk^3}\;\times$$

$$cosh[\,k(\xi-\xi_f)]\,H(\xi-\xi_f) - \frac{L^3}{2EIk^3}cos[\,k(\xi-\xi_f)]\,H(\xi-\xi_f)]$$

(5.17)

$$M(\xi,\xi_f) \;=\; \frac{EIk^2}{L^2}\big[-C_1\sin(k\xi) - C_2\cos(k\xi) \;+\; C_3\sinh(k\xi) \;+ C_4\cosh(k\xi) \;+$$

$$\frac{L^3}{2EIk^3} \times sinh[\,k(\xi-\xi_f)]\,H(\xi-\xi_f) + \frac{L^3}{2EIk^3}\,sin\,[\,k(\xi-\xi_f)]\,H(\xi-\xi_f)] \tag{5.18}$$

$$V(\xi,\xi_f) = \frac{EIk^3}{L^3}\big[-C_1\,cos\,(k\xi) + C_2\,sin\,(k\xi) + C_3 cosh\,(k\xi) + C_4\,sinh(k\xi) + \frac{L^3}{2EIk^3}\,cosh\big[\,k(\xi-\xi_f)\big]H(\xi-\xi_f) + \frac{L^3}{2EIk^3} cos\,[\,k(\xi-\xi_f)]\,H(\xi-\xi_f)]$$

(5.19)

The boundary conditions for this beam are

$$M\,(0,\ \xi_f) = k_{R1}\,\Psi\ (0,\ \xi_f) \tag{5.20a}$$

$$V\,(0,\ \xi_f) = -\,k_{T1}\ G\,(0,\ \xi_f) \tag{5.20b}$$

$$M\,(1,\ \xi_f) = -\,k_{R2}\,\Psi\ (1,\ \xi_f) \tag{5.20c}$$

$$V\,(1,\ \xi_f) = k_{T2}\ G\,(1,\ \xi_f) \tag{5.20d}$$

Plug Eqs. (5.16) to (5.19) into boundary conditions, we have:

$$\begin{bmatrix} k_{R1} & \frac{kEI}{L} & k_{R1} & -\frac{kEI}{L} \\ -\frac{EIk^3}{L^3} & k_{T1} & \frac{EIk^3}{L^3} & k_{T1} \\ -\frac{EIk^2}{L^2}sin(k) + k_{R2}\frac{k}{L}cos(k) & -\frac{EIk^2}{L^2}cos(k) - k_{R2}\frac{k}{L}sin(k) & \frac{EIk^2}{L^2}sinh(k) + k_{R2}\frac{k}{L}cosh(k) & \frac{EIk^2}{L^2}cosh\,(k) + k_{R2}\frac{k}{L}sinh(k) \\ -\frac{EIk^3}{L^3}cos(k) - k_{T2}sin(k) & \frac{EIk^3}{L^3}sin(k) - k_{T2}cos(k) & \frac{EIk^3}{L^3}cosh(k) - k_{T2}sinh(k) & \frac{EIk^3}{L^3}sinh(k) - k_{T2}cosh(k) \end{bmatrix}$$

$$\times \begin{bmatrix} C_1 \\ C_2 \\ C_3 \\ C_4 \end{bmatrix} = \begin{bmatrix} 0 \\ 0 \\ -\frac{L}{2k}\sinh\big[\,k(1-\xi_f)\big] - \frac{L}{2k}\sin\big[\,k(1-\xi_f)\big] - \frac{k_{R2}L^2}{2EIk^2}\cosh\big[k(1-\xi_f)\big] + \frac{k_{R2}L^2}{2EIk^2}\cos\big[k(1-\xi_f)\big] \\ -\frac{L^3}{2EIk^3}sinh\big[k(1-\xi_f)\big] + \frac{L^3}{2EIk^3}sin\big[k(1-\xi_f)\big] - \frac{1}{2}\cosh\big[k(1-\xi_f)\big] - \frac{1}{2}\cos\big[k(1-\xi_f)\big] \end{bmatrix}$$

(5.21)

5.3 Forced Vibration of Simply Supported Euler-Bernoulli Beams

In this section, the forced vibration curve of a simply supported Euler-Bernoulli beam under a moving delta load is derived.

For simply supported beam, the four boundary conditions are

$$G(0,\ \xi_f) = 0, G(1,\ \xi_f) = 0$$
$$M(0,\ \xi_f) = 0, M(1,\ \xi_f) = 0 \tag{5.22}$$

Plug Eqs. (5.16) and (5.18) into boundary conditions. Eq. (5.22) can be written as:

$$\begin{bmatrix} 0 & \frac{kEI}{L} & 0 & -\frac{kEI}{L} \\ 0 & 1 & 0 & 1 \\ -\frac{kEI}{L}sin(k) & -\frac{kEI}{L}cos(k) & \frac{kEI}{L}sinh(k) & \frac{kEI}{L}cosh(k) \\ sin(k) & cos(k) & sinh(k) & cosh(k) \end{bmatrix} \times \begin{bmatrix} C_1 \\ C_2 \\ C_3 \\ C_4 \end{bmatrix}$$
$$= \begin{bmatrix} 0 \\ 0 \\ -\frac{L}{2k}sinh[k(1-\xi_f)] - \frac{L}{2k}sin[k(1-\xi_f)] \\ -\frac{L^3}{2EIk^3}sinh[k(1-\xi_f)] + \frac{L^3}{2EIk^3}sin[k(1-\xi_f)] \end{bmatrix} \tag{5.23}$$

Eq. (5.21) describes a set of four nonhomogeneous equations of a general Timoshenko beam. When k_{R1} and k_{R2} equal to zero, k_{T1} and k_{T2} approach infinity, the general beam becomes a simply supported beam. Eq. (5.21) can be reduced to:

$$\begin{bmatrix} 0 & \frac{kEI}{L} & 0 & -\frac{kEI}{L} \\ 0 & 1 & 0 & 1 \\ -\frac{kEI}{L}sin(k) & -\frac{kEI}{L}cos(k) & \frac{kEI}{L}sinh(k) & \frac{kEI}{L}cosh\,(k) \\ sin(k) & cos(k) & sinh(k) & cosh(k) \end{bmatrix} \times \begin{bmatrix} C_1 \\ C_2 \\ C_3 \\ C_4 \end{bmatrix}$$

$$= \begin{bmatrix} 0 \\ 0 \\ -\frac{L}{2k}sinh[\,k(1-\xi_f)] - \frac{L}{2k}sin[\,k(1-\xi_f)] \\ -\frac{L^3}{2EIk^3}sinh[\,k(1-\xi_f)] + \frac{L^3}{2EIk^3}sin[\,k(1-\xi_f)\,] \end{bmatrix}$$

(5.24)

Eq. (5.24) matches Eq. (5.23), and can be validated by a simply supported beam.

CHAPTER 6 Forced Vibrations of Timoshenko Beams

6.1 Deflection Curves of Forced Vibrations of Timoshenko Beams

The governing equations for forced vibration of Timoshenko beams are:

$$EI\frac{\partial^2\varphi}{\partial x^2}+KAG\left(\frac{\partial y}{\partial x}-\varphi\right)-\rho I\frac{\partial^2\varphi}{\partial t^2}=0 \tag{6.1}$$

$$-\rho A\frac{\partial^2 y}{\partial t^2}+KAG\left(\frac{\partial^2 y}{\partial x^2}-\frac{\partial\varphi}{\partial x}\right)=-q(x,t) \tag{6.2}$$

where *q(x,t)* is the applied exciting distributed load function pointing upwards. It can be written as

$$q(\xi,t)=exp(i\omega_\omega t)\ \delta\ (\xi-\xi_f) \tag{6.3}$$

where ξ is the dimensionless length *x*/L.

After applying separation of variable, Eqs. (6.1) and (6.2) become

$$EI\frac{\partial^4 y}{\partial x^4}+\rho A\frac{\partial^2 y}{\partial t^2}-\left(\frac{EI\rho}{KG}+\rho I\right)\frac{\partial^4 y}{\partial x^2\partial t^2}+\rho I\frac{\rho}{KG}\frac{\partial^4 y}{\partial t^4}=\ q(x,t)-\frac{EI}{KGA}\frac{\partial^2 q}{\partial x^2}\ +\frac{I\rho}{KGA}\frac{\partial^2 q}{\partial t^2} \tag{6.4}$$

$$EI\frac{\partial^4\varphi}{\partial x^4}\ +\ \rho A\frac{\partial^2\varphi}{\partial t^2}-\left(\frac{EI\rho}{KG}+\ \rho I\right)\frac{\partial^4\varphi}{\partial x^2\partial t^2}+\rho I\frac{\rho}{KG}\frac{\partial^4\varphi}{\partial t^4}=\frac{\partial q(x,t)}{\partial x} \tag{6.5}$$

The deflection shapes for forced vibrations of a Timoshenko beam can be defined as a Green function

$$y(\xi,t)\ =\ Y(\xi,\xi_f)\ exp(i\omega_\omega t) \tag{6.6}$$

where ξ_f is the point where the arbitrary force is applied at.

$Y(\xi, \xi_f)$ has two components, a general solution to the homogenous equations and a particular solution to the nonhomogeneous equations.

$$Y(\xi, \xi_f) = Y_0(\xi) + Y_1(\xi, \xi_f) H(\xi - \xi_f) \tag{6.7}$$

From chapter 4, the homogenous solution has been given

$$Y_0(\xi) = C_1 \cosh(b\alpha\xi) + C_2 \sinh(b\alpha\xi) + C_3 \cos(b\beta\xi) + C_4 \sin(b\beta\xi) \tag{6.8}$$

$$\Psi_0(\xi) = D_1 \sinh(b\alpha\xi) + D_2 \cosh(b\alpha\xi) + D_3 \sin(b\beta\xi) + D_4 \cos(b\beta\xi) \tag{6.9}$$

Substitute Eqs. (6.6) and (6.7) into Eq. (6.4), and omit $exp(i\omega_\omega t)$ on both sides of equation. Eq. (6.4) can be written as:

$$\frac{d^4Y(\xi,\xi_f)}{d\xi^4} + \frac{L^2\omega_\omega{}^2\rho(1+\frac{E}{Gk})}{E} \frac{d^2Y(\xi,\xi_f)}{d\xi^2} + \frac{L^4\omega^2(\rho^2\omega_\omega{}^2\frac{I}{Gk}-\rho A)}{EI} Y(\xi, \xi_f) =$$

$$-\frac{L^2}{GkA}\frac{d^2\delta(\xi-\xi_f)}{d\xi^2} + \frac{L^4}{EI}\left(1-\frac{I\rho\omega_\omega{}^2}{GkA}\right)\delta(\xi-\xi_f) \tag{6.10}$$

From section 4.1, we know

$$b^2 = \rho A L^4 \omega_\omega{}^2 / (EI) \tag{6.11}$$

$$r^2 = I / (AL^2) \tag{6.12}$$

$$s^2 = EI / (KAGL^2) \tag{6.13}$$

Eq. (6.10) can be written as

$$Y^{IV} + b^2(r^2+s^2)Y'' - b^2(1-r^2s^2b^2)Y = \frac{(1-b^2r^2s^2)L^4}{EI}\delta(\xi-\xi_f) -$$

$$\frac{L^4s^2}{EI}\delta''(\xi-\xi_f) \tag{6.14}$$

The damping effect is neglected in this thesis, which may cause large errors for the vibration curves at high frequencies. The mode shape functions derived in this chapter are just for dimensionless frequencies *b*, lower than cut-off frequency ($b < \frac{1}{r^2 s^2}$).

The particular solution to the nonhomogeneous Eq. (6.14) has the following format,

$$Y_1(\xi, \xi_f) = P_1 \cosh[b\alpha(\xi - \xi_f)] + P_2 \sinh[b\alpha(\xi - \xi_f)] + P_3 \cos[b\beta(\xi - \xi_f)] + P_4 \sin[b\beta(\xi - \xi_f)] \quad (6.15)$$

P_1 to P_4 can be determined by the continuity conditions. The continuity conditions are listed below:

$$Y(\xi_f{}^+, \xi_f) - Y(\xi_f{}^-, \xi_f) = 0 \quad (6.16a)$$

$$\Psi(\xi_f{}^+, \xi_f) - \Psi(\xi_f{}^-, \xi_f) = 0 \quad (6.16b)$$

$$M(\xi_f{}^+, \xi_f) - M(\xi_f{}^-, \xi_f) = 0 \quad (6.16c)$$

$$V(\xi_f{}^+, \xi_f) - V(\xi_f{}^-, \xi_f) = 1 \quad (6.16d)$$

Eqs. (6.1) and (6.2) can be rewritten in term of *b*, *r*, and *s* as:

$$s^2\Psi'' - (1 - b^2 r^2 s^2)\Psi + Y'/L = 0 \quad (6.17)$$

$$Y'' + b^2 s^2 Y - L\Psi' = \frac{\delta(\xi - \xi_f)L^2}{KAG} \quad (6.18)$$

From Eq. (6.18), Ψ' can be written as

$$\Psi' = \frac{Y'' + b^2 s^2 Y}{L} - \frac{\delta(\xi - \xi_f)\mathrm{L}}{\mathrm{KAG}} \quad (6.19)$$

Ψ'' can be calculated by

$$\Psi'' = \frac{Y''' + b^2 s^2 Y'}{L^2} - \frac{\delta'(\xi - \xi_f)}{KAG} \tag{6.20}$$

From Eq. (6.17), we get

$$\Psi = (s^2 \Psi'' + \frac{Y'}{L}) / (1 - b^2 r^2 s^2) \tag{6.21}$$

Plug Eq. (6.20) into Eq. (6.21)

$$\Psi = (\frac{s^2 Y^{'''} + b^2 s^4 Y'}{L^2} - \frac{\delta'(\xi - \xi_f) s^2}{\mathrm{KAG}} + \frac{Y'}{L}) / (1 - b^2 r^2 s^2) \tag{6.22}$$

For Timoshenko beams, the moment can be calculated by

$$M = EI\Psi' \tag{6.23}$$

Plug Eq. (6.19) in to Eq. (6.23), then M can rewritten as

$$M = EI(\frac{Y'' + b^2 s^2 Y}{L} - \frac{\delta(\xi - \xi_f)\mathrm{L}}{\mathrm{KAG}}) \tag{6.24}$$

Shear force can be obtained by

$$V = -KAG\big(Y'(\xi, \xi_f) - \Psi(\xi, \xi_f)\big) \tag{6.25}$$

Plug Eq. (6.22) into Eq. (6.25), then shear force can be stated as

$$V = -KAG[Y' - (\frac{s^2 Y^{'''} + b^2 s^4 Y'}{L^2} - \frac{\delta'(\xi - \xi_f) s^2}{\mathrm{KAG}} + \frac{Y'}{L}) / (1 - b^2 r^2 s^2)\ ] \tag{6.26}$$

Plug in Eqs. (6.22), (6.24), and (6.26) to the continuity conditions. After simplifying, the continuity conditions can be written as:

$$Y_1(\xi_f, \xi_f) = 0 \tag{6.27a}$$

$$(b^2 s^4 + L) Y_1'(\xi_f, \xi_f) + s^2 Y_1'''(\xi_f, \xi_f) = 0 \tag{6.27b}$$

$$Y_1''(\xi_f, \xi_f) + b^2 s^2 Y_1(\xi_f, \xi_f) = 0 \tag{6.27c}$$

$$\frac{-KAG}{L^2(b^2 r^2 - 1/s^2)} [(b^2 r^2 L + b^2 s^2) Y_1'(\xi_f, \xi_f) - Y_1'''(\xi_f, \xi_f)] = 1 \tag{6.27d}$$

P_1 to P_4 can be obtained by solving Eqs. (6.27a) to (6.27d). We get

$$P_1 = P_3 = 0$$

$$P_2 = \frac{L(1 - b^2 s^2 r^2 - b^2 s^2 \alpha^2)}{KAG b^3 s^2 \alpha(\alpha^2 + \beta^2)}$$

$$P_4 = -\frac{L(1 - b^2 s^2 r^2 + b^2 s^2 \beta^2)}{KAG b^3 s^2 \beta(\alpha^2 + \beta^2)} \tag{6.28}$$

In conclusion, the vibration shapes for forced vibrations of Timoshenko beams can be stated as

$$Y(\xi) = C_1 \cosh(b\alpha\xi) + C_2 \sinh(b\alpha\xi) + C_3 \cos(b\beta\xi) + C_4 \sin(b\beta\xi) +$$

$$\frac{L(1 - b^2 s^2 r^2 - b^2 s^2 \alpha^2)}{KAG b^3 s^2 \alpha(\alpha^2 + \beta^2)} \times sinh[b\alpha(\xi - \xi_f)] - \frac{L(1 - b^2 s^2 r^2 + b^2 s^2 \beta^2)}{KAG b^3 s^2 \beta(\alpha^2 + \beta^2)} sin[b\beta(\xi - \xi_f)]$$

(6.29)

where α and β are defined as

$$\alpha = \sqrt{\frac{1}{2}[-(r^2 + s^2) + \sqrt{(r^2 - s^2)^2 + \frac{4}{b^2}}]} \tag{6.30}$$

$$\beta = \sqrt{\frac{1}{2}[(r^2 + s^2) + \sqrt{(r^2 - s^2)^2 + \frac{4}{b^2}}]} \tag{6.31}$$

Deflection Y, and bending slope Ψ can be written as

$$Y(\xi, \xi_f) = C_1 \cosh(b\alpha\xi) + C_2 \sinh(b\alpha\xi) + C_3 \cos(b\beta\xi) + C_4 \sin(b\beta\xi) +$$

$$P_2 \sinh[b\alpha(\xi - \xi_f)] + P_4 \sin[b\beta(\xi - \xi_f)] \tag{6.32}$$

$$\Psi(\xi, \xi_f) = D_1 \sinh(b\alpha\xi) + D_2 \cosh(b\alpha\xi) + D_3 \sin(b\beta\xi) + D_4 \cos(b\beta\xi) + M_2 \times$$

$$\cosh[b\alpha(\xi - \xi_f) + M_4 \cos[b\beta(\xi - \xi_f)] \tag{6.33}$$

The coefficients from Eq. (6.32), C_1 to P_4 can be related with the coefficients in Eq. (6.33), D_1 to M_4 by Eq. (6.5). We get

$$C_1 = \frac{L\alpha}{b(\alpha^2+s^2)} D_1 \qquad C_2 = \frac{L\alpha}{b(\alpha^2+s^2)} D_2$$

$$C_3 = -\frac{L\beta}{b(\beta^2-s^2)} D_3 \qquad C_4 = -\frac{L\beta}{b(\beta^2-s^2)} D_4$$

$$P_2 = \frac{L\alpha}{b(\alpha^2+s^2)} \mathrm{M}_2 \qquad P_4 = \frac{L\beta}{b(\beta^2-s^2)} M_4$$

$$M_2 = \frac{b(\alpha^2+s^2)}{L\alpha} \times \frac{1 - b^2s^2r^2 - b^2s^2\alpha^2}{KAGb^2s^2\alpha(\alpha^2+\beta^2)} \qquad M_4 = \frac{b(\beta^2-s^2)}{L\beta} \frac{1-b^2s^2r^2+b^2s^2\beta^2}{KAGb^2s^2\beta(\alpha^2+\beta^2)} \tag{6.34}$$

In summary, the bending angle Ψ can be written as

$$\Psi(\xi, \xi_f) = D_1 \sinh(b\alpha\xi) + D_2 \cosh(b\alpha\xi) + D_3 \sin(b\beta\xi) + D_4 \cos(b\beta\xi) +$$

$$\frac{\alpha^2+s^2}{\alpha} \times \frac{1 - b^2s^2r^2 - b^2s^2\alpha^2}{KAGb^2s^2\alpha(\alpha^2+\beta^2)} \cosh[b\alpha(\xi - \xi_f)] - \frac{\beta^2-s^2}{\beta} \frac{1-b^2s^2r^2+b^2s^2\beta^2}{KAGb^2s^2\beta(\alpha^2+\beta^2)} \cos[b\beta(\xi - \xi_f)]$$

(6.35)

6.2 Forced Vibrations of Timoshenko Beams with Two Different Rotational Springs and Two Different Vertical Springs

Free vibrations of the general Timoshenko beam with two different rotational springs and two different vertical springs are discussed in section 4.2. In this section, forced vibrations of the general Timoshenko beam are studied. To the best of my knowledge, dynamic response of the general beam has not been published in any literature yet.

The boundary conditions are

$$\begin{aligned} M\,(0,\xi_f) &= k_{R1}\Psi(0,\xi_f) \\ V(0,\xi_f) &= -k_{T1}Y\,(0,\xi_f) \\ M\,(1,\xi_f) &= -k_{R2}\Psi\,(1,\xi_f) \\ V(1,\xi_f) &= k_{T2}\,Y\,(1,\xi_f) \end{aligned} \tag{6.36}$$

Deflection Y, bending angle Ψ, and moment M, can be calculated by

$$Y(\xi,\xi_f) = \frac{L\alpha}{b(\alpha^2+s^2)}D_1 cosh\,(b\alpha\xi) + \frac{L\alpha}{b(\alpha^2+s^2)}D_2\,sinh\,(b\alpha\xi) - \frac{L\beta}{b(\beta^2-s^2)}D_3\,cos\,(b\beta\xi) + \frac{L\beta}{b(\beta^2-s^2)}D_4\,sin\,(b\beta\xi) + \frac{L\alpha}{b(\alpha^2+s^2)}M_2 sinh[b\alpha(\xi - \xi_f)] + \frac{L\beta}{b(\beta^2-s^2)}M_4\,sin[b\beta(\xi - \xi_f)] \tag{6.37}$$

$$\Psi(\xi,\xi_f) = D_1\,sinh\,(b\alpha\xi) + D_2\,cosh\,(b\alpha\xi) + D_3\,sin\,(b\beta\xi) + D_4\,cos\,(b\beta\xi) + M_2 cosh[b\alpha(\xi - \xi_f)] + M_4 cos[b\beta(\xi - \xi_f)] \tag{6.38}$$

$$M(\xi,\xi_f) = \frac{EIb\alpha}{L}\,cosh\,(b\alpha\xi)\,D_1 + \frac{EIb\alpha}{L}\,sinh\,(b\alpha\xi)D_2 + \frac{EIb\beta}{L}\,cos\,(b\beta\xi)D_3 - \frac{EIb\beta}{L}\,sin\,(b\beta\xi)D_4 + \frac{EIb\alpha}{L}M_2 sinh[b\alpha(\xi - \xi_f)] - \frac{EIb\beta}{L}M_4\,sin[b\beta(\xi - \xi_f)] \tag{6.39}$$

The shear force can be calculated as

$$V = -KAG\left(Y'(\xi,\xi_f) - \Psi(\xi,\xi_f)\right) \tag{6.40}$$

which can be re-written as

$$V = KAG\left(\frac{S^2}{\alpha^2+s^2}\sinh(b\alpha\xi)\,D_1 + \frac{S^2}{\alpha^2+s^2}\cosh(b\alpha\xi)\,D_2 - \frac{S^2}{\beta^2-s^2}\times\sin(b\beta\xi)\,D_3 - \frac{S^2}{\beta^2-s^2}\cos(b\beta\xi)D_4 + \frac{S^2}{\alpha^2+s^2}M_2\cosh[b\alpha(\xi - \xi_f)] - \frac{S^2}{\beta^2-s^2}M_4\,cos[b\beta(\xi - \xi_f)]\right. \tag{6.41}$$

Substitute Eqs. (6.39) to (6.41) into boundary conditions, one gets the following expression:

$$\begin{bmatrix} \frac{-k_{T1}L\alpha}{b(\alpha^2+s^2)} & \frac{-KAGs^2}{(\alpha^2+s^2)} & \frac{k_{T1}L\beta}{b(\beta^2-s^2)} & \frac{KAGs^2}{(\beta^2-s^2)} \\ \frac{EIb\alpha}{L} & -k_{R1} & \frac{EIb\beta}{L} & -k_{R1} \\ \frac{\mathrm{KAG}s^2 b\sinh(b\alpha)-k_{T2}L\alpha\cosh(b\alpha)}{b(\alpha^2+s^2)} & \frac{KAGs^2 b\cosh(b\alpha)-k_{T2}L\alpha\sinh(\mathrm{b}\alpha)}{b(\alpha^2+s^2)} & \frac{-\mathrm{KAG}s^2 b\sin(\mathrm{b}\beta)+k_{T2}L\beta\cos(b\alpha)}{b(\beta^2-s^2)} & \frac{-\mathrm{KAG}s^2 b\cos(\mathrm{b}\beta)-k_{T2}L\beta\sin(b\alpha)}{b(\beta^2-s^2)} \\ \frac{EIb\alpha\cosh(b\alpha)+k_{R2}Ls\sinh(\mathrm{b}\alpha)}{L} & \frac{EIb\alpha\sinh(b\alpha)+k_{R2}Lcos\mathrm{h}(\mathrm{b}\alpha)}{L} & \frac{EIb\beta\cos(b\alpha)+k_{R2}Ls\sin(\mathrm{b}\alpha)}{L} & \frac{-EIb\beta\sin(b\alpha)+k_{R2}Lcos(\mathrm{b}\alpha)}{L} \end{bmatrix} \times \begin{bmatrix} D_1 \\ D_2 \\ D_3 \\ D_4 \end{bmatrix} =$$

$$\begin{bmatrix} 0 \\ 0 \\ \frac{-KAGs^2}{\alpha^2+s^2}\,\mathrm{M}_2\cosh[b\alpha(1-\xi_f)] + \frac{KAGs^2}{\beta^2-s^2}M_4\cos[b\beta(1-\xi_f)] + \frac{L\alpha}{b(\alpha^2+s^2)}k_{T2}\mathrm{M}_2\sinh[b\alpha(1-\xi_f)] + \frac{L\beta}{b(\beta^2-s^2)}M_4\,k_{T2}\sin[b\beta(1-\xi_f) \\ -\frac{EIb\alpha}{L}M_2 sinh[b\alpha(1-\xi_f)] + \frac{EIb\beta}{L}M_4\,sin[b\beta(1-\xi_f)] - k_{R2}M_2 cosh[b\alpha(1-\xi_f)] - k_{R2}\,M_4 cos[b\beta(1-\xi_f)] \end{bmatrix} \tag{6.42}$$

6.3 Forced Vibrations of Simply Supported Timoshenko Beams

Forced vibration deflection shape of a simply supported Timoshenko beam is calculated in this chapter. The boundary conditions of a simply supported beam are

$$Y(0,\ \xi_f) = 0,\ Y(1,\xi_f)\ = 0$$
$$M\ (0,\xi_f)\ = 0, M\ (1,\xi_f)\ = 0 \tag{6.43}$$

Apply Eq. (6.37) and Eq. (6.39) into boundary conditions,

$$\begin{bmatrix} \frac{L\alpha}{b(\alpha^2+s^2)} & 0 & -\frac{L\beta}{b(\beta^2-s^2)} & 0 \\ \frac{EIb\alpha}{L} & 0 & \frac{EIb\beta}{L} & 0 \\ \frac{L\alpha}{b(\alpha^2+s^2)}cosh(b\alpha) & \frac{L\alpha}{b(\alpha^2+s^2)}sinh(b\alpha) & -\frac{L\beta}{b(\beta^2-s^2)}cos(b\beta) & \frac{L\beta}{b(\beta^2-s^2)}sin(b\beta) \\ \frac{EIb\alpha}{L}cosh(b\alpha) & \frac{EIb\alpha}{L}sinh(b\alpha) & \frac{EIb\beta}{L}cos(b\beta) & -\frac{EIb\beta}{L}sin(b\beta) \end{bmatrix} \times \begin{bmatrix} D_1 \\ D_2 \\ D_3 \\ D_4 \end{bmatrix} =$$
$$\begin{bmatrix} 0 \\ 0 \\ -\frac{L\alpha}{b(\alpha^2+s^2)}M_2sinh[b\alpha(1-\ \xi_f)] - \frac{L\beta}{b(\beta^2-s^2)}M_4sin[b\beta(1-\ \xi_f)] \\ -\frac{EIb\alpha}{L}M_2sinh\big[b\alpha\big(1-\ \xi_f\big)\big] + \frac{EIb\beta}{L}M_4sin[b\beta(1-\ \xi_f)] \end{bmatrix} \tag{6.44}$$

When k_{R1} and k_{R2} equal to zero, k_{T1} and k_{T2} reach infinity, the general beam studied in section 6.2 becomes a simply supported beam. Eq. (6.42) can be simplified to

$$\begin{bmatrix} \frac{L\alpha}{b(\alpha^2+s^2)} & 0 & -\frac{L\beta}{b(\beta^2-s^2)} & 0 \\ \frac{EIb\alpha}{L} & 0 & \frac{EIb\beta}{L} & 0 \\ \frac{L\alpha}{b(\alpha^2+s^2)}cosh(b\alpha) & \frac{L\alpha}{b(\alpha^2+s^2)}sinh(b\alpha) & -\frac{L\beta}{b(\beta^2-s^2)}cos(b\beta) & \frac{L\beta}{b(\beta^2-s^2)}sin(b\beta) \\ \frac{EIb\alpha}{L}cosh(b\alpha) & \frac{EIb\alpha}{L}sinh(b\alpha) & \frac{EIb\beta}{L}cos(b\beta) & -\frac{EIb\beta}{L}sin(b\beta) \end{bmatrix} \times \begin{bmatrix} D_1 \\ D_2 \\ D_3 \\ D_4 \end{bmatrix} = \begin{bmatrix} 0 \\ 0 \\ -\frac{L\alpha}{b(\alpha^2+s^2)}M_2 sinh[b\alpha(1-\xi_f)] - \frac{L\beta}{b(\beta^2-s^2)}M_4 sin[b\beta(1-\xi_f)] \\ -\frac{EIb\alpha}{L}M_2 sinh\left[b\alpha\left(1-\xi_f\right)\right] + \frac{EIb\beta}{L}M_4 sin[b\beta(1-\xi_f)] \end{bmatrix} \quad (6.45)$$

Therefore, Eq. (6.42), describing the boundary conditions of the general beam model, is verified with Eq. (6.45). The simple beam case expressed in Eq. (6.45) is identical to that derived by Lueschen et al. (1996).

CHAPTER 7 Results and Discussion

7.1 Comparison of Natural Frequencies between Euler-Bernoulli Beams and Timoshenko Beams under Free Vibrations

To verify accuracy of the numerical derivation of natural frequencies in this thesis, a cantilever beam with a rotational spring constraint is studied using Euler-Bernoulli beam theory and Timoshenko beam theory. The results are compared with Chen and Kiriakidis's (2005) results. The boundary conditions for the beam are k_{T1} approaches infinity, k_{R2} and k_{T2} equal to zero. Below is the sketch of the beam:

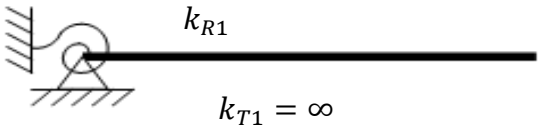

Figure 7.1: A Cantilever Beam with a Rotational Spring

The properties of the beam are listed in Table 7.1:

A = 15.71 cm^2	E = 5.72× 10^4 MPa	$\rho = 1976\ kg/m^3$	K = 0.56
E/KG = 4.29	r = 0.012	L = 1.5 m	

Table 7.1: Beam Properties for the Numerical Example in Section 7.1

Define two new variables: dimensionless rotational spring constant *k*^, and dimensionless frequency *γ*. *k*^ and γ can be calculated as,

$$\gamma^4 = \frac{\rho A L^4 \omega^2}{EI} \tag{7.1}$$

$$k\hat{} = \frac{k_{R1}L}{EI} \qquad (7.2)$$

Dimensionless frequency of the Euler-Bernoulli beam γ, and natural frequency ratio of the Timoshenko beam to the Euler-Bernoulli beam f_T/f_{EB}, are summarized using Table 7.2. The dimensionless frequencies of first five modes ($\gamma_1, \gamma_2, \gamma_3, \gamma_4, \gamma_5$) are all smaller than the dimensionless cut off frequency 3352.

Case	γ_1	f_T/f_{EB}	γ_2	f_T/f_{EB}	γ_3	f_T/f_{EB}	γ_4	f_T/f_{EB}	γ_5	f_T/f_{EB}
Hinge-free (k^= 0)	3.927	0.994	7.069	0.982	10.21	0.964	13.35	0.940	16.49	0.913
k^=1	1.248	0.999	4.031	0.994	7.134	0.982	10.26	0.963	13.39	0.940
k^=10	1.723	0.999	4.402	0.991	7.451	0.978	10.52	0.959	13.61	0.936
k^=100	1.857	0.997	4.650	0.986	7.783	0.970	10.90	0.950	14.01	0.928
Fixed-free (k^=∞)	1.875	0.997	4.694	0.986	7.855	0.969	11.00	0.947	14.14	0.924

Table 7.2: Comparison of Frequency Ratio (f_T/f_{EB}) between Timoshenko Beam and Euler-Bernoulli Beam with Various Boundary Conditions

The results matches Chen and Kiriakidis's (2005) results very well. Chen and Kiriakidis's results are tabulated in Table 7.3.

Case	γ_1	f_T/f_{BE}	γ_2	f_T/f_{BE}	γ_3	f_T/f_{BE}	γ_4	f_T/f_{BE}	γ_5	f_T/f_{BE}
Hinge-free ($K\hat{} = 0$)	3.927	0.994	7.069	0.982	10.21	0.964	13.35	0.940	16.49	0.913
$K\hat{} = 1$	1.248	0.999	4.031	0.994	7.134	0.982	10.26	0.963	13.39	0.940
$K\hat{} = 10$	1.723	0.999	4.402	0.991	7.451	0.978	10.52	0.959	13.61	0.936
$K\hat{} = 100$	1.857	0.997	4.650	0.986	7.783	0.970	10.90	0.950	14.01	0.928
Fixed-free ($K\hat{} = \infty$)	1.875	0.997	4.694	0.986	7.855	0.969	11.00	0.947	14.14	0.924

Table 7.3: Chen and Kiriakidis's Results for Comparison of Frequency Ratio (f_T/f_{EB}) between Timoshenko Beam and Euler-Bernoulli Beam with Various Boundary Conditions

From Table 7.2, conclusions can be drawn that when dimensionless rotational spring $k\hat{}$ increases, the natural frequency increases. The ratio of natural frequency for the Timoshenko beam to natural frequency for the Euler-Bernoulli beam becomes smaller at higher modes. Natural

frequencies at lower modes are more sensitive to boundary restraints than natural frequencies at higher modes.

Furthermore, the frequency ratio of mode *m* to mode *n* for Euler-Bernoulli beams is independent of the material properties and dimensions of the beam, but the frequency ratio is dependent on the boundary constraints, $k\hat{}$. However, the frequency ratio of mode *m* to mode *n* for Timoshenko beams is dependent on the materials properties, dimensions, and dimensionless rotational spring constant $k\hat{}$. For the same boundary conditions, natural frequency of the Timoshenko beam is always less than the natural frequency of the Euler-Bernoulli beam, because of the shear deformation and rotatory inertia effects.

In Table 7.2, the inverse slenderness ratio *r* is fixed at 0.012. Figure 7.2 shows the frequency ratio f_T/f_{EB} (natural frequency of the Timoshenko beam to natural frequency of the Euler-Bernoulli beam) with three $k\hat{}$ values, versus dimensionless inverse slenderness ratio *r* for the first three modes. It is worth noting that the frequecy ratio f_T/f_{EB} at higher modes drops more rapidly as *r* increases. The boundary restraints $k\hat{}$, and f_T/f_{EB} has a negative relationship.

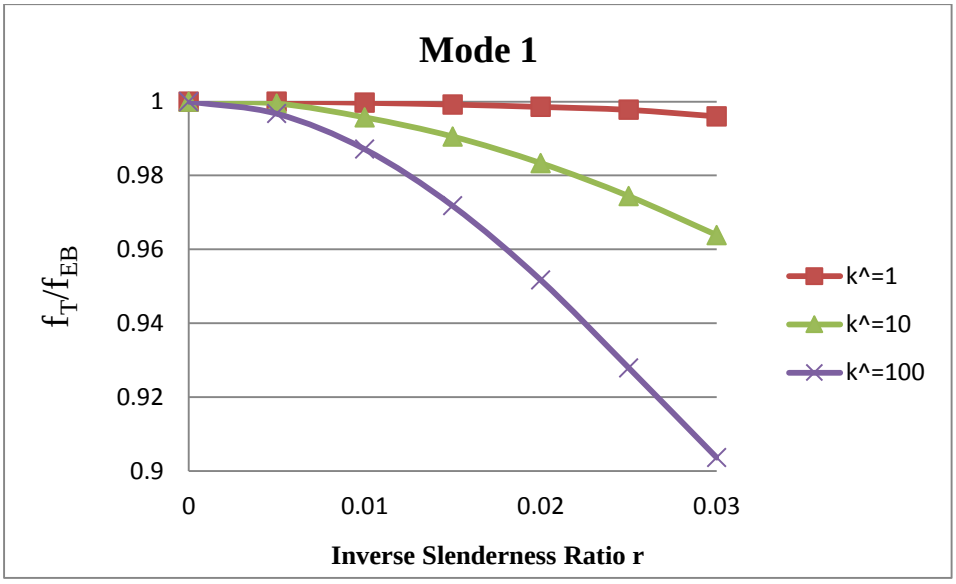

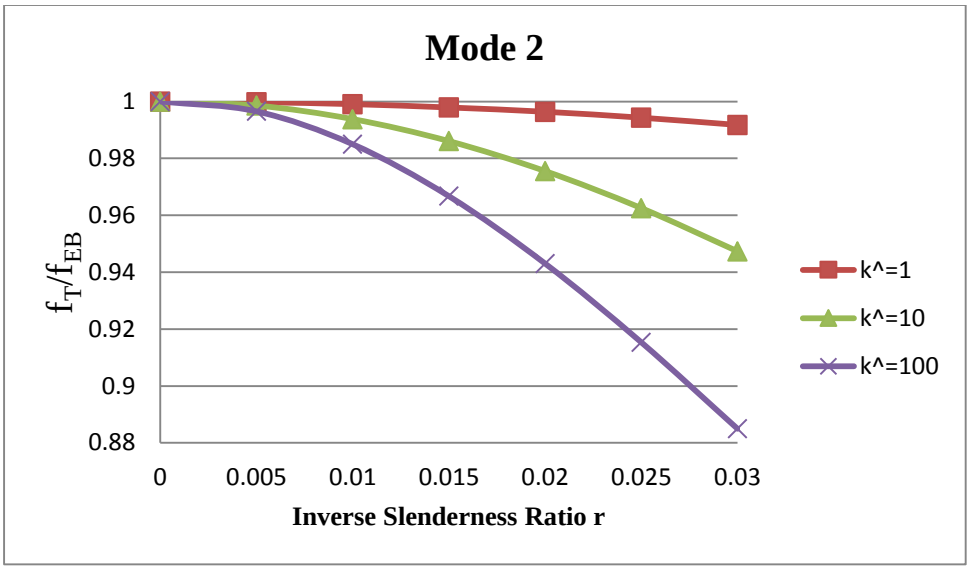

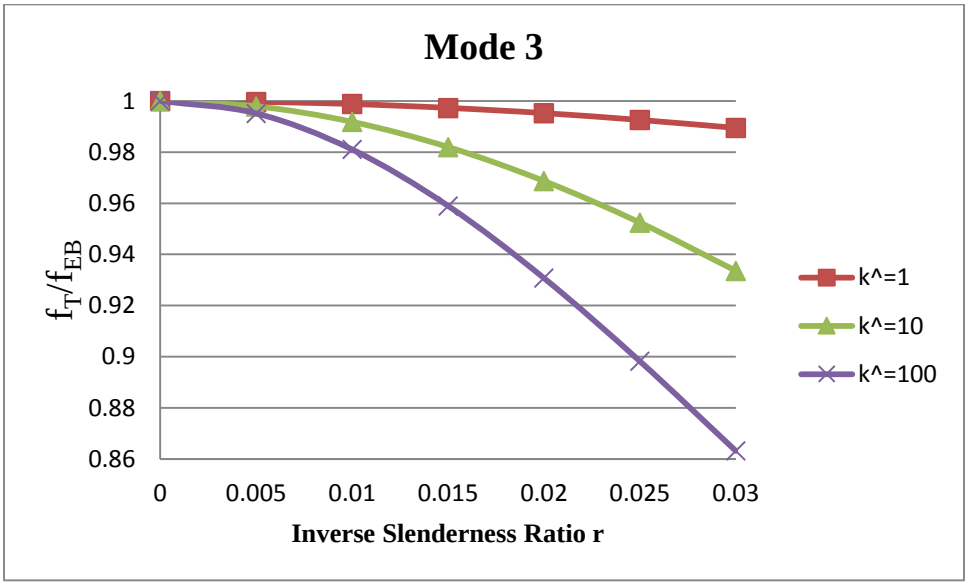

Figure 7.2: Frequency Ratio (f_T/f_{EB}) between Timoshenko Beam and Euler-Bernoulli Beam Due to Different *k*^, and Dimensionless Inverse Ratio *r*

7.2 Comparison of Mode Shapes between Euler-Bernoulli Beams and Timoshenko Beams under Free Vibrations

7.2.1 Mode shapes Comparison of a Cantilever Beam under Free Vibration

In this section, comparison of mode shapes between an Euler-Bernoulli beam and a Timoshenko beam is presented. The numerical example used in this section is the same as Huang's (1961) example. The beam properties are summarized in Table 7.4:

$A = 1\ in^2$	$E = 3\times 10^7 psi$	$\gamma = 0.28\ lb/in^3$	$K = 2/3$
$E/G = 8/3$	$r = 0.02$	$L = 14.4\ in$	$S = 0.04$

Table 7.4: Beam Properties for the Numerical Example in section 7.2.1

When the beam is a cantilever beam, mode shapes of the Euler-Bernoulli beam and the Timoshenko beam have been derived in section 3.2, and section 4.3, respectively. The dimensionless cut off frequency for the beam is 1250. The dimensionless natural frequencies of the first five modes for the Euler-Bernoulli beam are 1.87, 4.69, 7.85, 11.00, and 14.14, which are smaller than the cut off frequency. The dimensionless natural frequencies of the first five modes for the Timoshenko beam are 1.87, 4.62, 7.58, 10.34, and 12.91, which are also smaller than the cut off frequency.

Figure 7.3 shows the first five mode shapes for the Euler-Bernoulli beam, which can be generated using the MATLAB program in Appendix III. Blue line represents the mode shape of the first mode. Red line represents the mode shape of the second mode. Yellow line represents the mode shape of the third mode. Green line represents the mode shape of the fourth mode. Black line represents the mode shape of the mode. Each mode shape is reduced in the way that the coefficient of hyperbolic cosine equals to 1**.**

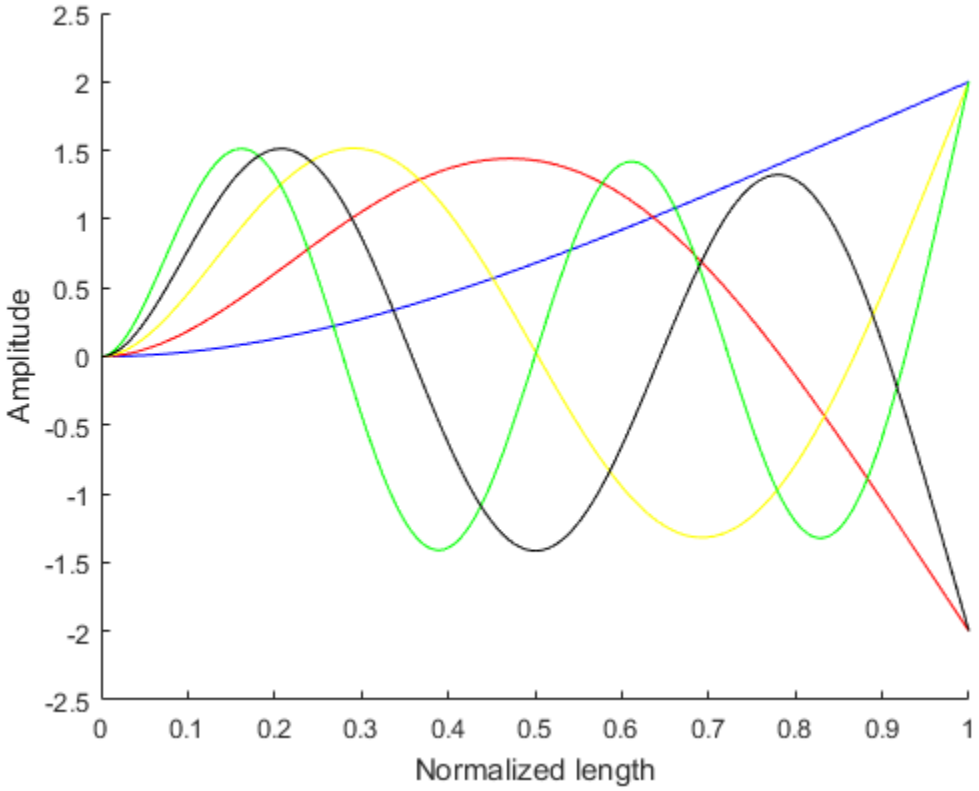

Figure 7.3: First Five Mode Shapes for a Cantilever Euler-Bernoulli beam

Figure 7.4 sketches the first five modes shapes for the Timoshenko beam. The mode shapes can be determined using the MATLAB program in Appendix IV. Each mode shape is reduced in the way that the coefficient of hyperbolic cosine equals to 1.

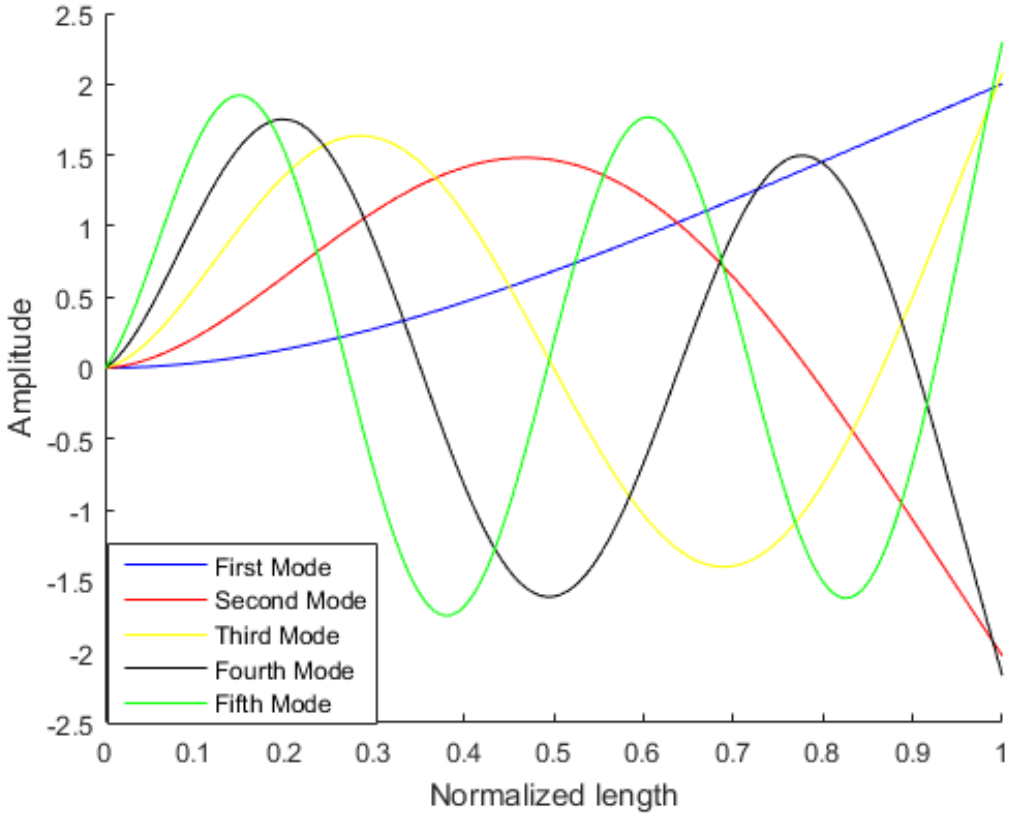

Figure 7.4: First Five Mode Shapes of a Cantilever Timoshenko Beam

Figure 7.5 illustrates the comparison of the superimposed mode shape amplitude of the first five modes for the Euler-Bernoulli beam and the Timoshenko beam.

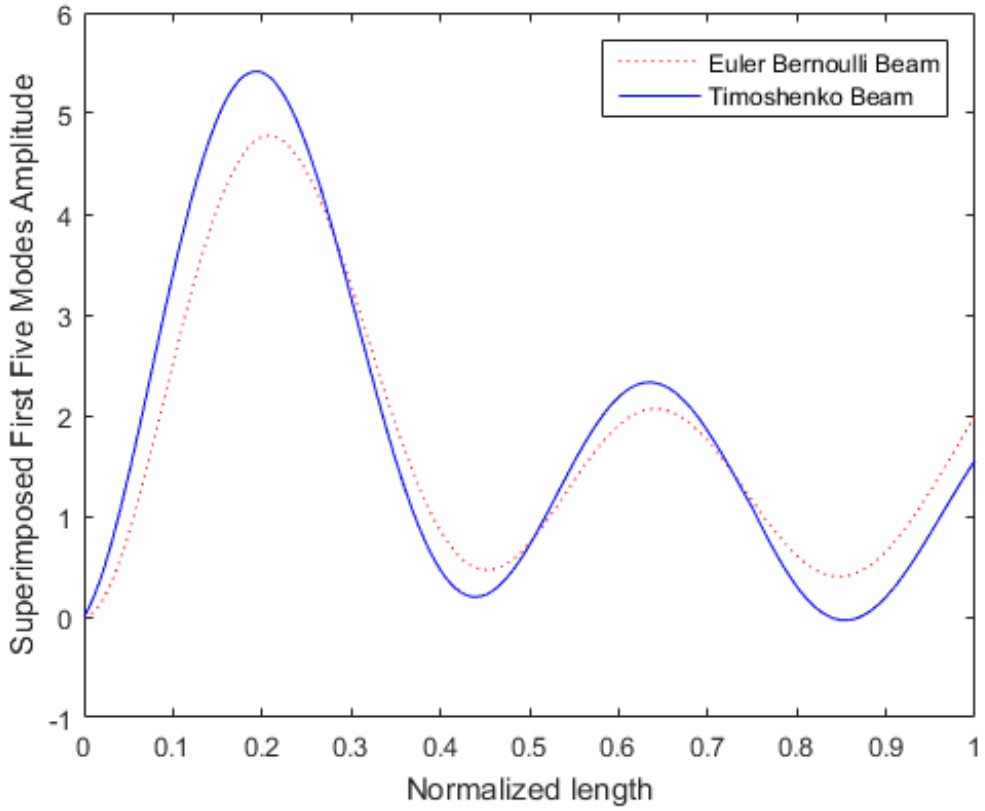

Figure 7.5: Comparison of Superimposed Mode Shapes for a Cantilever Beam

Figure 7.5 are reproduced and compared with Huang's (1961) plot, as shown in Figure 7.6. Dashed line represents the superimposed mode shape for the Euler-Bernoulli beam, and continuous line denotes the superimposed mode shape for the Timoshenko beam in Figure 7.6. It can be seen that the results are matched well.

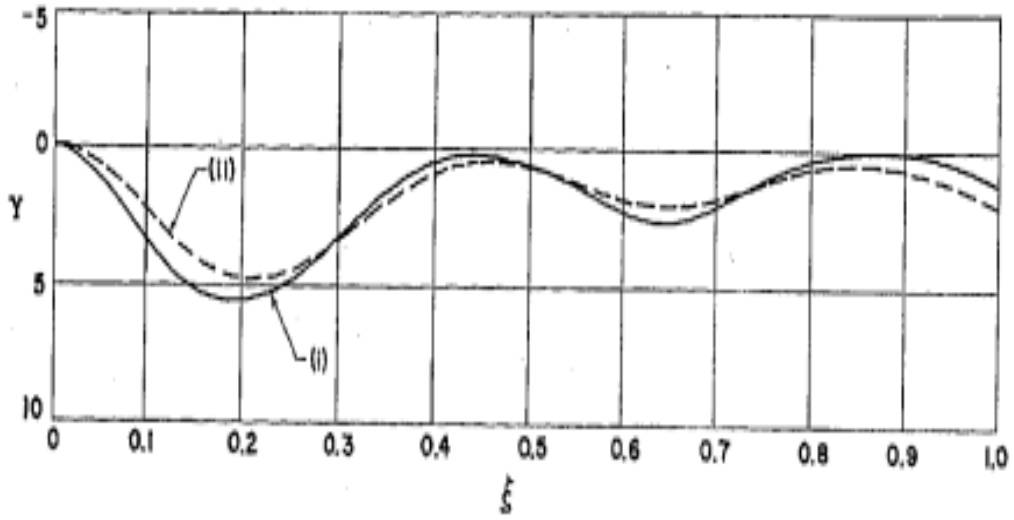

Figure 7. 6(a): Huang's (1961) Results for Superimposed Mode Shapes for a Cantilever Beam (Dashed Line: Euler-Bernoulli Beam, Continuous Line: Timoshenko Beam)

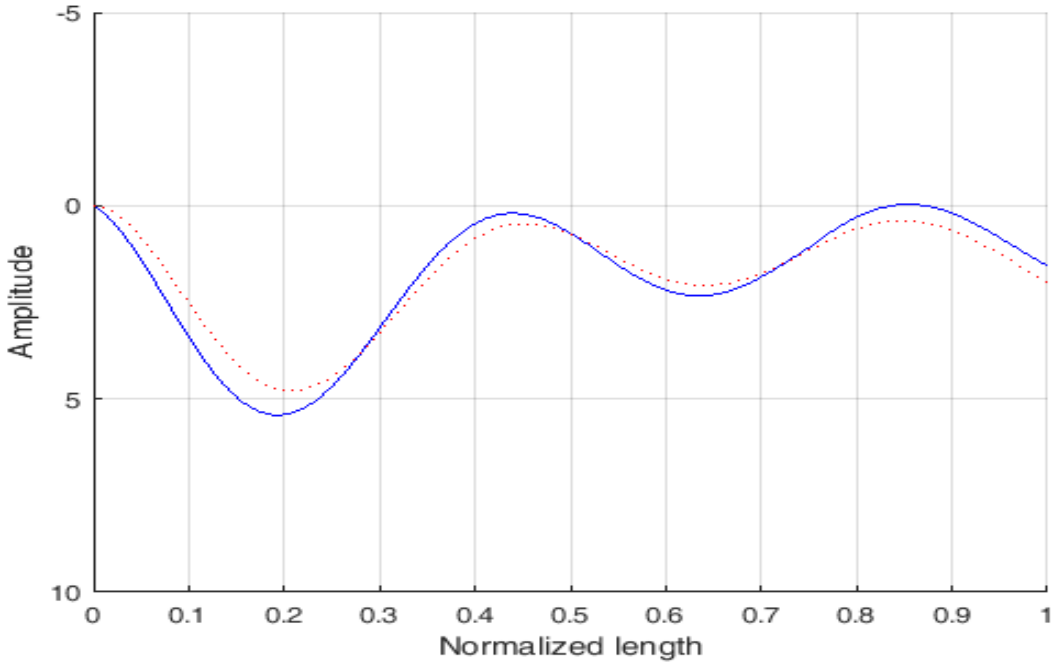

Figure 7.6(b): Superimposed Mode Shapes for a Cantilever Beam from This Thesis (Dashed Line: Euler-Bernoulli Beam, Continuous Line: Timoshenko Beam)

7.2.2 Comparison of Mode Shapes of a Beam with Two Fixed Vertical Supports and Two Rotational Springs under Free Vibrations

In this section, mode shapes of a beam with two fixed vertical supports and two rotational springs at both ends are presented using Euler-Bernoulli beam theory and Timoshenko beam theory. Below is the sketch of the beam:

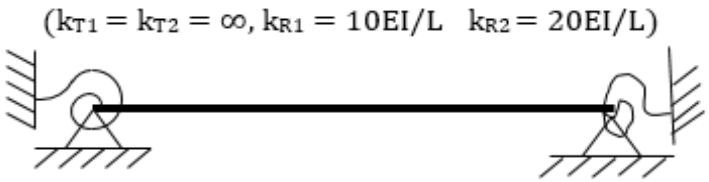

Figure 7.7: A Beam with Two Different Rotational Springs

Same numerical example is used as the example in section 7.2.1. Beam properties can be found in Table 7.4. The boundary conditions of the beam are given by:

$$k_{T1} = k_{T2} = \infty$$

$$k_{R1} = \frac{10EI}{L}, k_{R2} = \frac{20EI}{L} \tag{7.3}$$

The dimensionless cut off frequency for the beam equals 1250. The dimensionless natural frequencies of the first five modes for the Euler-Bernoulli beam are 4.25, 7.14, 10.06, 12.92, and 15.71. The dimensionless natural frequencies of the first five modes for the Timoshenko beam are 4.20, 6.98, 9.67, 12.23, and 14.63. The dimensionless natural frequencies of the first five modes for the Euler-Bernoulli beam and the Timoshenko beam are smaller than the cut off frequency.

By running the MATLAB file in Appendix III, the first five mode shapes for Euler-Bernoulli beam are generated, as shown in Figure 7.8. Each mode shape is reduced in the way that the coefficient of hyperbolic cosine equals to 1.

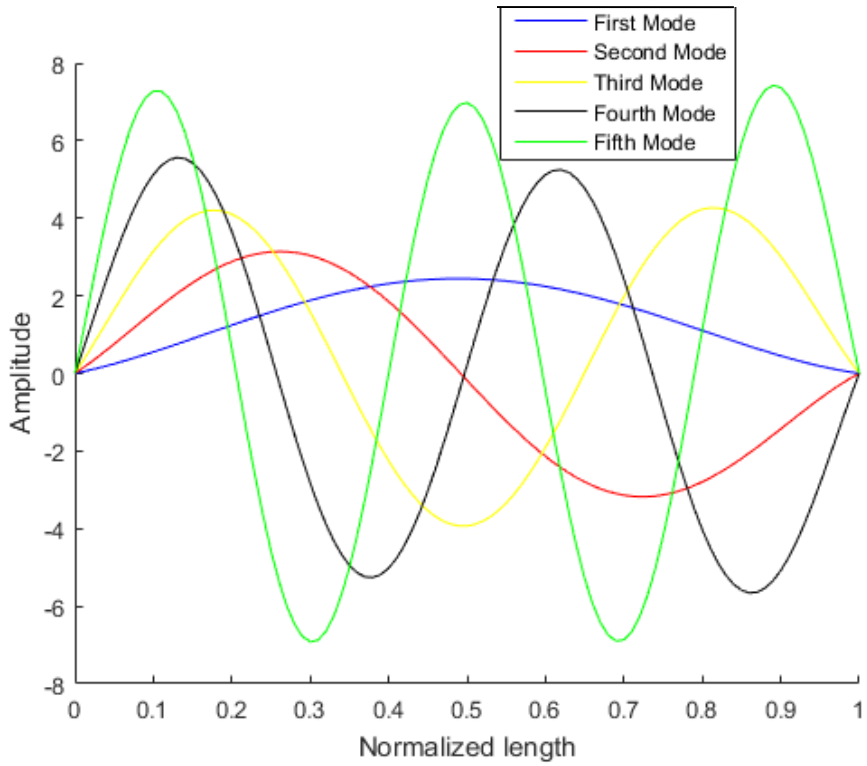

Figure 7.8: First Five Modes Shapes for an Euler-Bernoulli Beam with Two Different Rotational Springs

From Appendix IV, the first five mode shapes for the Timoshenko beam can be obtained by inputting beam properties and boundary conditions. Each mode shape is reduced in the way that the coefficient of hyperbolic cosine equals to 1.

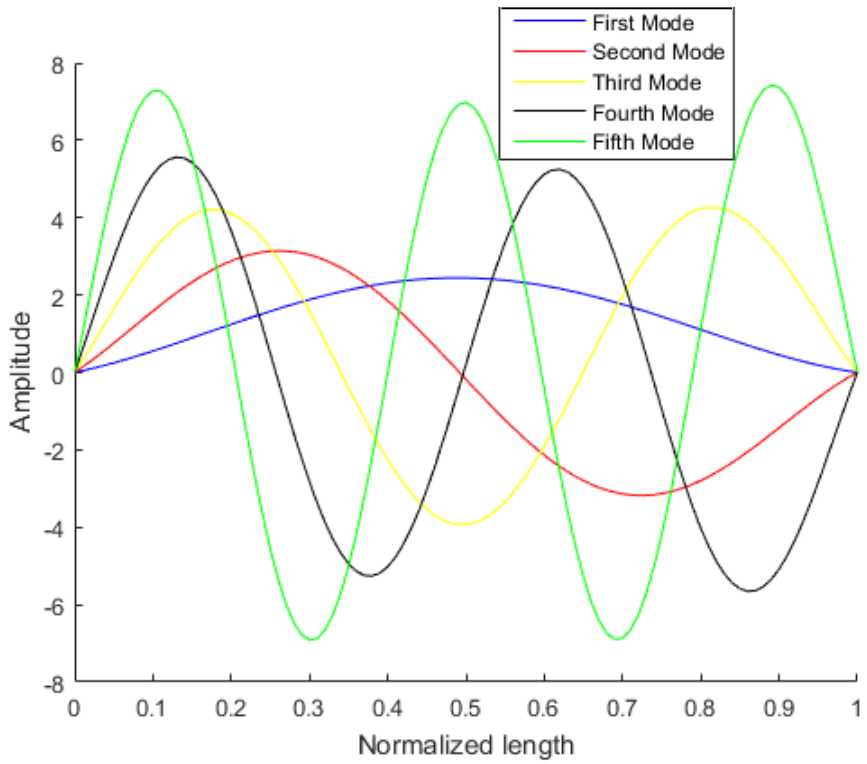

Figure 7.9: First Five Modes Shapes for a Timoshenko beam with Two Different Rotational Springs

Figure 7.10 illustrates the comparison of superimposed first five modes between the Euler-Bernoulli beam and the Timoshenko beam. The red dashed line represents the superimposed mode shape for the Euler-Bernoulli beam. The blue solid line shows the superimposed mode shape for the Timoshenko Beam.

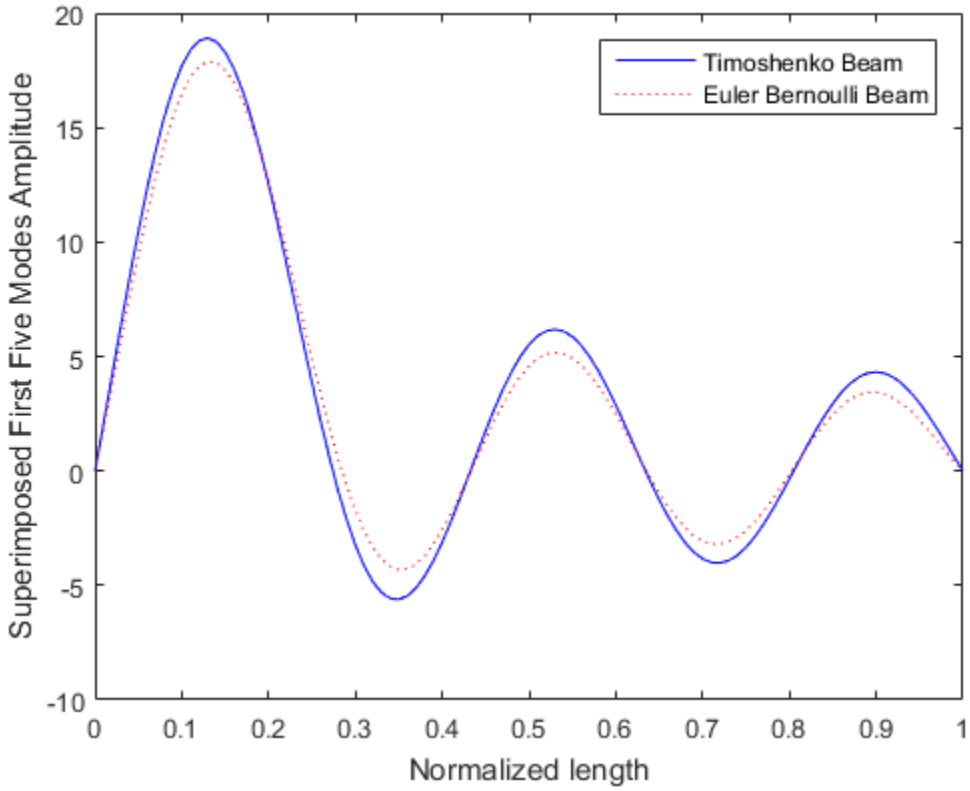

Figure 7.10: Comparison of Superimposed Mode Shapes for a Beam with Two Different Rotational Springs

7.3 Deflection Curves Comparison of Forced Vibrations

7.3.1 Deflection Curves of a Simply Supported Beam under Forced Vibrations

In this section, comparison of deflection curves between an Euler-Bernoulli beam and a Timoshenko beam under forced vibration of a moving delta load is presented with numerical calculation. Using the same numerical examples as presented in Lueschen's (1996) paper, the beam properties are summarized in Table 7.5:

$A = 4\ in^2$	$E = 3\times 10^7 psi$	$\rho = 7.28 \times 10^{-4} lb/in^3$	$K = 0.83$
$E/G = 8/3$	$v = 0.3$	$L = 20\ in$	$I = 1.33\ in^4$

Table 7.5: Beam Properties for the Numerical Example in 7.3.1 and 7.3.2

A delta load is located at the mid-span of the simply supported beam. The cut off frequency is 25965 Hz. When the frequencies of the applied harmonic load equal to 100 Hz, 1700 Hz, 3000 Hz, and14000 Hz, the deflection curves for the Euler-Bernoulli beam and the Timoshenko beam are plotted in Figure 7.11

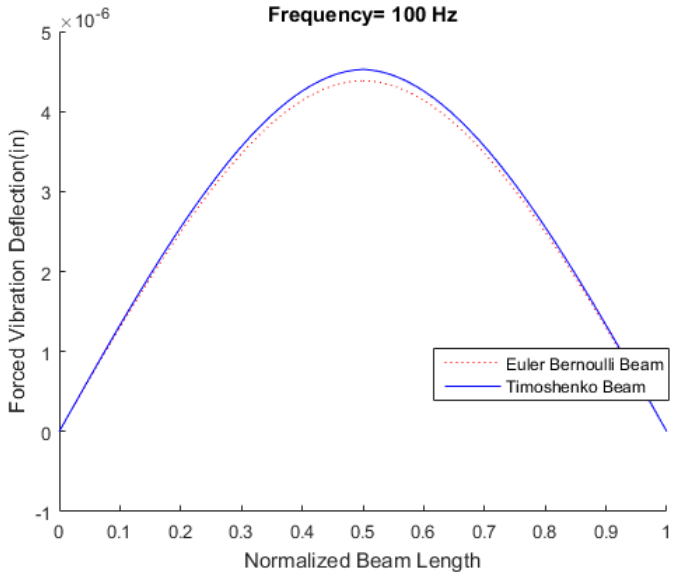

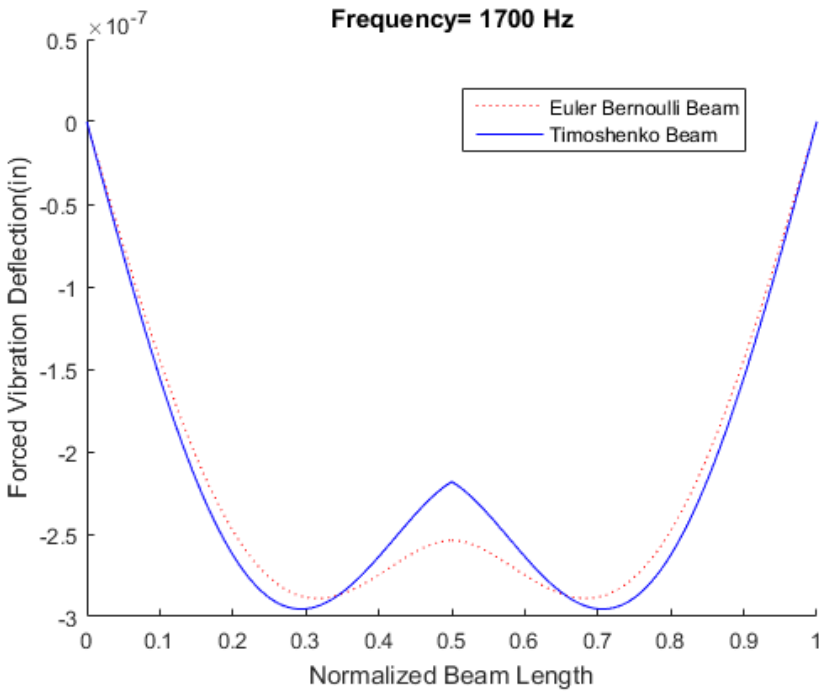
Frequency= 1700 Hz
×10^-7
0.5
0
-0.5
-1
-1.5
-2
-2.5
-3
Forced Vibration Deflection(in)
Euler Bernoulli Beam
Timoshenko Beam
0
0.1
0.2
0.3
0.4
0.5
0.6
0.7
0.8
0.9
1
Normalized Beam Length

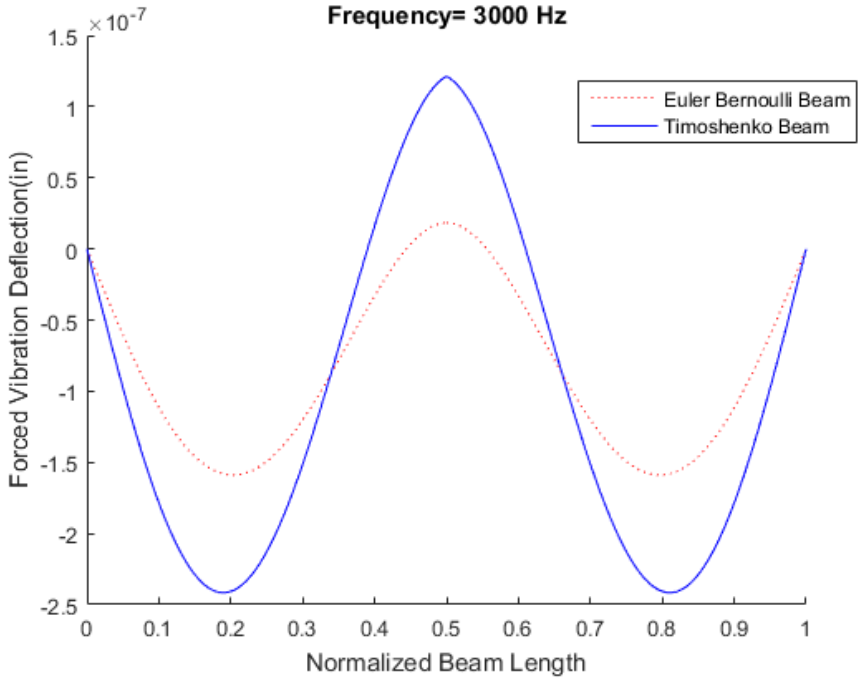
Frequency= 3000 Hz
×10^-7
1.5
1
0.5
0
-0.5
-1
-1.5
-2
-2.5
Forced Vibration Deflection(in)
Euler Bernoulli Beam
Timoshenko Beam
0
0.1
0.2
0.3
0.4
0.5
0.6
0.7
0.8
0.9
1
Normalized Beam Length

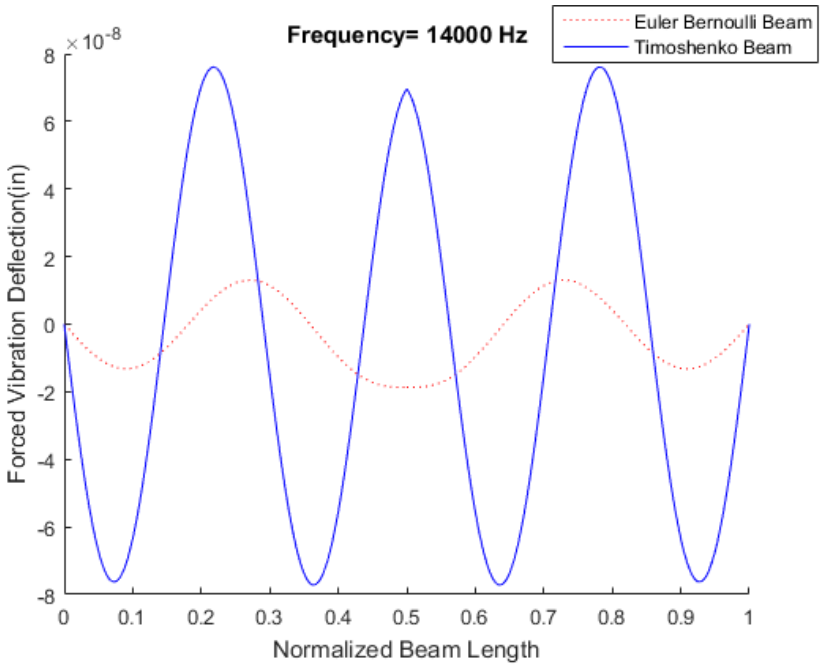

Figure 7.11: Comparison of Deflection Curves of a Simply Supported Beam under Forced Vibrations

From Figure 7.11, the deflection of the Timoshenko beam is always greater than the deflection of the Euler-Bernoulli beam. Also, the deflection difference becomes larger at higher frequencies.

The deflection curves presented by Lueschen et al (1996) are shown in Figure 7.12. It can be seen that Figure 7.11 results match closely with Lueschen's (1996) plots, as illustrated in Figure 7.12 with the frequencies of the applied harmonic load equal to (a) 100 Hz, (b) 1700 Hz, (c) 3000 Hz, and (d) 14000 Hz.

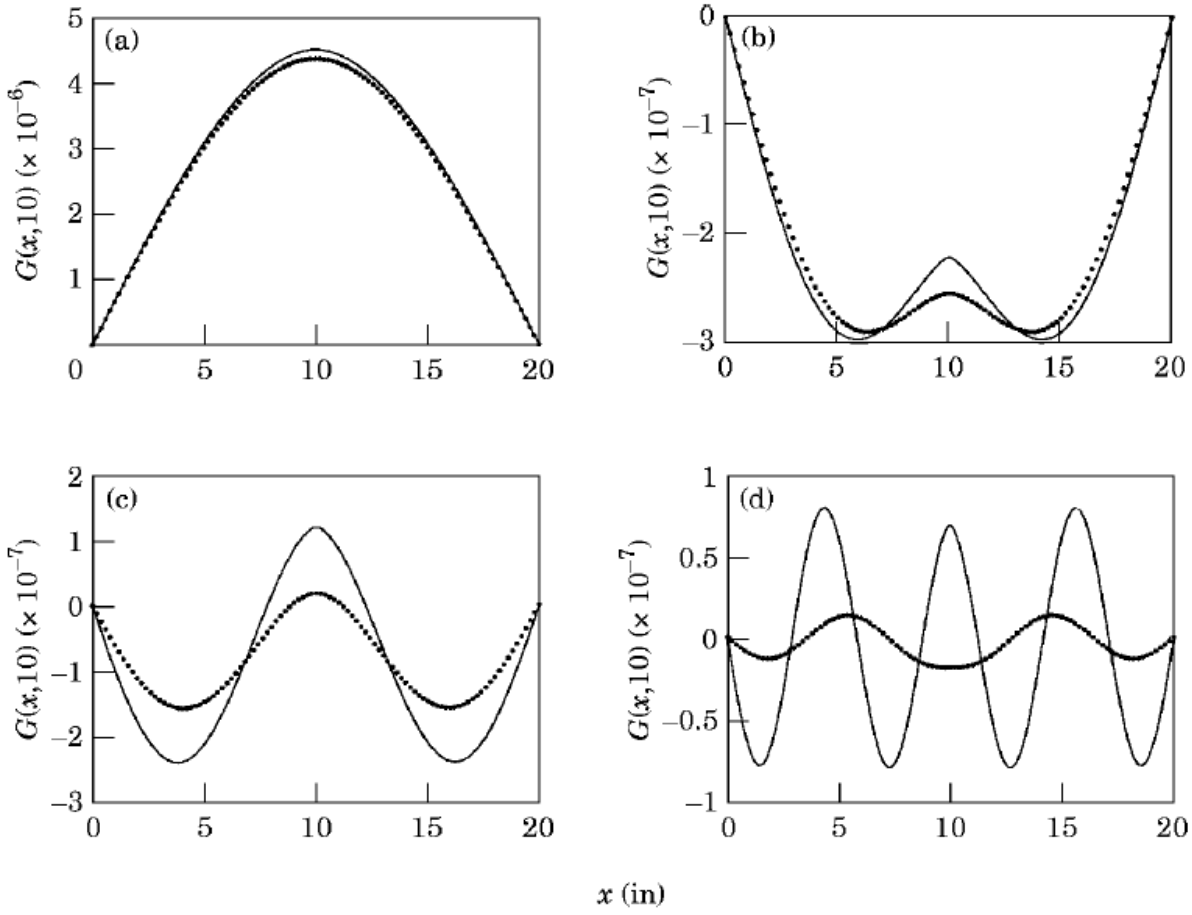

Figure 7.12: Deflection Curves of a Simply Supported Beam under Forced Vibrations from Lueschen et al. (1996), (Solid Line - Timoshenko Beam and Dotted Line - Euler Bernolli Beam)

7.3.2 Deflection Curves of a Beam with Two Fixed Vertical Supports and Two Rotational Springs under Forced Vibrations

In this section, deflection curves comparison of a beam with two fixed vertical supports and two rotational springs under a moving delta load using Euler-Bernoulli beam theory and Timoshenko beam is illustrated. The boundary conditions are shown as Figure 7.7. The boundary conditions of the beam are given by $k_{T1} = k_{T2} = \infty$ and $k_{R1} = \frac{10EI}{L}, k_{R2} = \frac{20EI}{L}$.

The beam properties are summarized in Table 7.5. A delta load is located at the mid-span of the beam. The cut off frequency is 25965 Hz. When the frequencies of the applied harmonic load equal to 100 Hz, 1700 Hz, 3000 Hz, and14000 Hz, the deflection curves for the Euler-Bernoulli beam and the Timoshenko beam can be plotted in Figure 7.13.

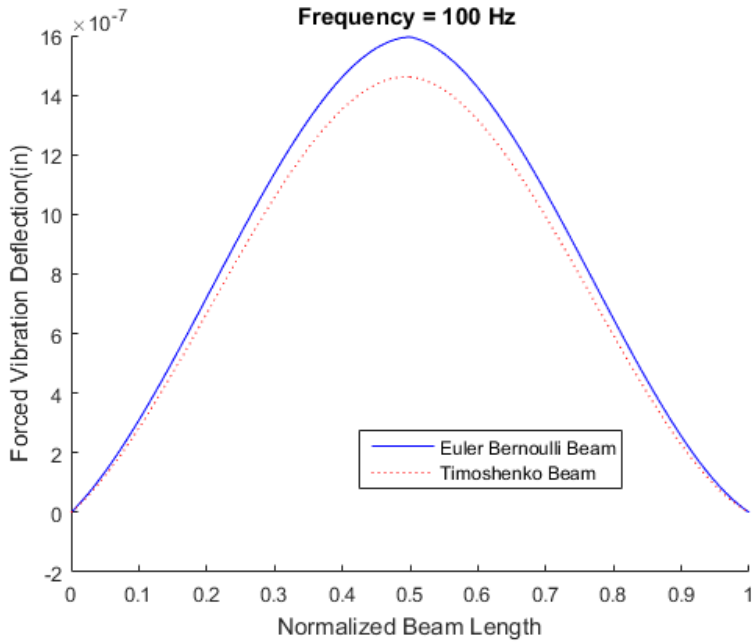

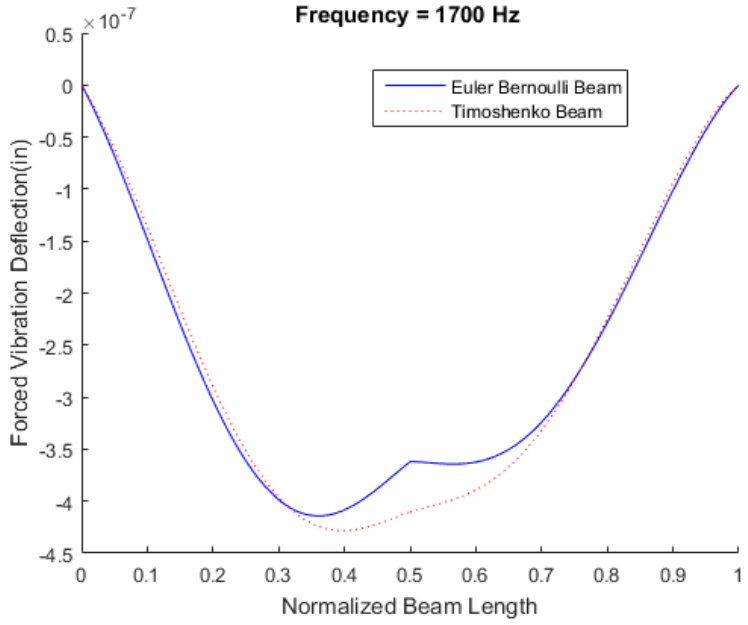

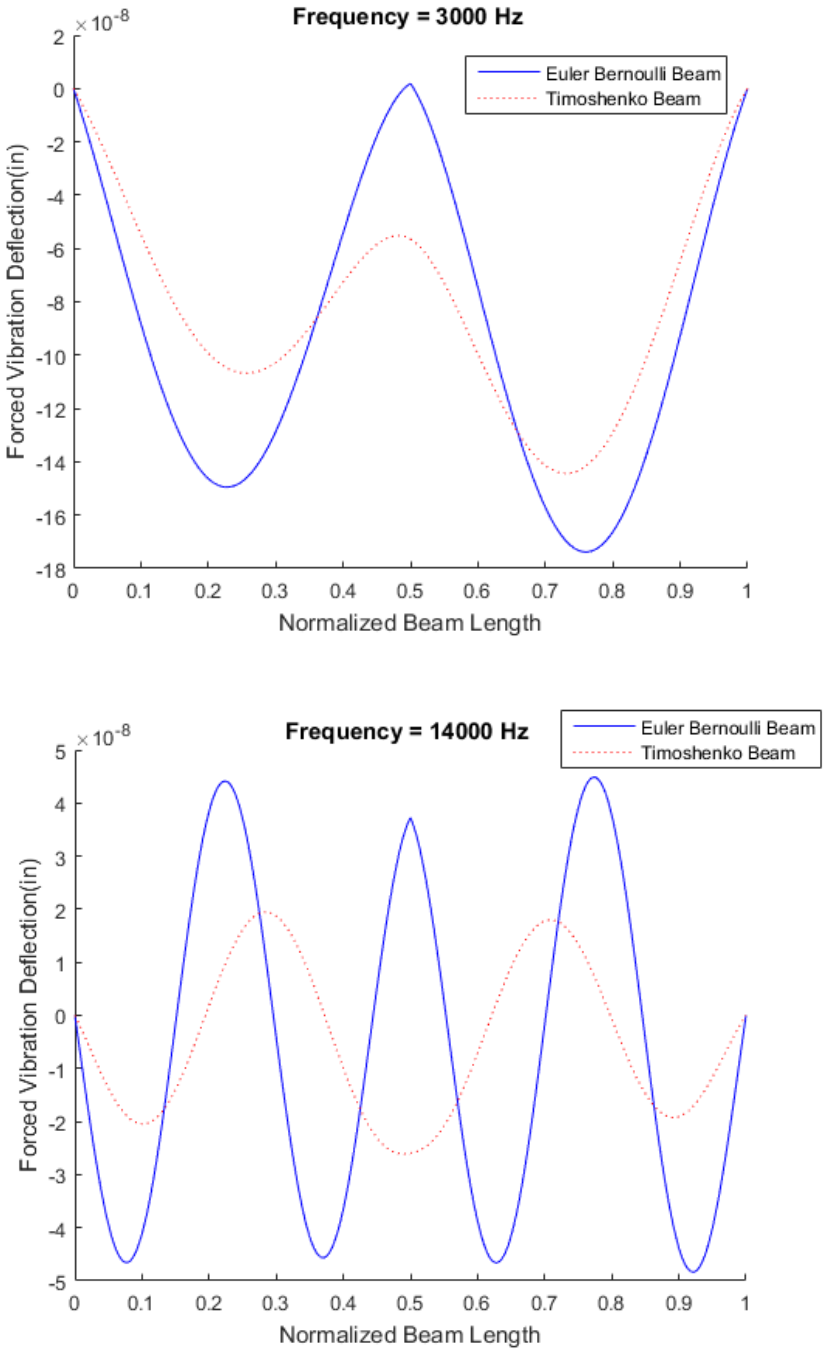

Figure 7.13: Comparison of Deflection Curves of a Beam with Two Rotational Springs under Forced Vibrations

It can be seen from the results that the deflection shapes are not symmetric when the loading frequencies are low, because the rotational springs at two ends are different. However, the deflection shapes tend to become symmetric at high loading frequencies. The influence of the boundary constraints becomes smaller when the loading frequency becomes higher.

It is worth noting that when the loading frequency reaches 14000 Hz, the Euler-Bernoulli beam and the Timoshenko beam vibrate at different modes. The natural frequency of the fifth mode of the Euler-Bernoulli beam is 12327 Hz, and the natural frequency of the seventh mode of the Timoshenko beam is 14592 Hz. Therefore, the Euler-Bernoulli beam vibrates at the fifth mode, and the Timoshenko beam vibrates at the seventh mode. The deflection shapes of the beam with harmonic excitation at 14000 Hz shown in Figure 7.11, 7.12 and 7.13 display this behavior.

Chapter 8 Conclusions and Recommendations

8.1 Conclusions

This study presents the derivation of natural frequencies and modes shapes of uniform Euler-Bernoulli beams and Timoshenko beams with various boundary conditions under free vibration using Eigenvalues and Eigenvectors. Furthermore, dynamic Green's functions and Fourier Transform are used to determine the deflection curve for forced vibrations of Euler-Bernoulli beams and Timoshenko beams. A general solution for a Timoshenko beam that can be applied to any arbitrary combinations of boundary conditions is derived, and to the best of our knowledge, this solution is not available in the literature. In this study, the transverse vibrations of Euler Bernoulli beams and Timoshenko beams using a general and direct beam model with two different rotational springs and two different vertical springs at the ends are analyzed, and the close-form solutions are presented. Numerical examples are presented to illustrate the differences in the natural frequencies and the mode shapes between Euler-Bernoulli beams and Timoshenko beams under free vibrations. Various boundary conditions can be achieved by assigning different values to the four spring constants. The ratio of the natural frequency of the Timoshenko beam to the natural frequency of the Euler-Bernoulli beams decreases at the higher modes. Natural frequencies at the lower modes are more sensitive to the boundary restraints than the natural frequencies at the higher modes.

8.2 Recommendations

The forced vibrations of uniform Euler-Bernoulli beams and Timoshenko beams are analyzed with the assumption that internal damping and external damping are neglected. The damping influence can cause a large error for the deflection amplitudes. The properties of the beam are constants in this thesis, such as the Young's modulus *E*, moment of inertia *I*, and cross section area *A*. For future study, damping effects and variations of beam properties should be included. In addition, dynamic responses of beams supported by an elastic foundation can be an interesting topic for future study.

References

Abu-Hilal, M. "Forced vibration of Euler–Bernoulli beams by means of dynamic Green functions." *Journal of sound and vibration* 267, no. 2 (2003): 191-207.

Azam, S. Eftekhar, M. Mofid, and R. Afghani Khoraskani. "Dynamic response of Timoshenko beam under moving mass." *Scientia Iranica* 20, no. 1 (2013): 50-56.

Challis, L., and Sheard, F. "The Green of Green Functions" *Physics Today* 56 (2003), 41-46.

Chen, Hung-Liang Roger, and Alejandro C. Kiriakidis. "Nondestructive evaluation of ceramic candle filter with various boundary conditions." *Journal of Nondestructive Evaluation* 24, no. 2 (2005): 67-81.

Chen, Hung-Liang Roger, and Alejandro C. Kiriakidis. "Stiffness evaluation and damage detection of ceramic candle filters." *Journal of engineering mechanics*126, no. 3 (2000): 308-319.

Ekwaro-Osire, S., D. H. S. Maithripala, and J. M. Berg. "A series expansion approach to interpreting the spectra of the Timoshenko beam." *Journal of sound and Vibration* 240, no. 4 (2001): 667-678.

Esmailzadeh, Ebrahim, and Mehrdaad Ghorashi. "Vibration analysis of a Timoshenko beam subjected to a travelling mass." *Journal of Sound and Vibration* 199, no. 4 (1997): 615-628.

Foda, M. A., and Z. Abduljabbar. "A dynamic Green function formulation for the response of a beam structure to a moving mass." *Journal of sound and vibration* 210, no. 3 (1998): 295-306.

Hamada, T. R. "Dynamic analysis of a beam under a moving force: a double Laplace transform solution." *Journal of Sound and Vibration* 74, no. 2 (1981): 221-233.

Huang, T. C. "The effect of rotatory inertia and of shear deformation on the frequency and normal mode equations of uniform beams with simple end conditions." *Journal of Applied Mechanics* 28, no. 4 (1961): 579-584.

Li, X. Y., X. Zhao, and Y. H. Li. "Green's functions of the forced vibration of Timoshenko beams with damping effect." *Journal of Sound and Vibration* 333, no. 6 (2014): 1781-1795.

Lueschen, G. G. G., L. A. Bergman, and D. M. McFarland. "Green's functions for uniform Timoshenko beams." *Journal of Sound and Vibration* 194, no. 1 (1996): 93-102.

Mackertich, Seroj. "Response of a beam to a moving mass." *The Journal of the Acoustical Society of America* 92, no. 3 (1992): 1766-1769.

Majkut, Leszek. "Free and forced vibrations of Timoshenko beams described by single differential equation." *Journal of Theoretical and Applied Mechanics*: 193-210.

Mehri, B. A. H. M. A. N., A. Davar, and O. Rahmani. "Dynamic Green function solution of beams under a moving load with different boundary conditions."*Scientia iranica* 16, no. 3 (2009): 273-279.

Mohamad, A. S. "Tables of Green's functions for the theory of beam vibrations with general intermediate appendages." *International journal of solids and structures* 31, no. 2 (1994): 257-268.

Radovizky, R., (2013). Simple Beam Theory. http://web.mit.edu/16.20/homepage/7_SimpleBeamTheory/SimpleBeamTheory_files/module_7_with_solutions.pdf.

Rayleigh, John William Strutt Baron. *The theory of sound*. Vol. 2. Macmillan, 1896.

Roshandel, D., M. Mofid, and A. Ghannadiasl. "Modal analysis of the dynamic response of Timoshenko beam under moving mass." *Scientia Iranica. Transaction A, Civil Engineering* 22, no. 2 (2015): 331.

Ross, Timothy J., and Felix S. Wong. "Timoshenko beams with rotational end constraints." *Journal of engineering mechanics* 111, no. 3 (1985): 416-430.

Timoshenko, S. P. "On the correction factor for shear of the differential equation for transverse vibrations of prismatic bar." *Philosophical Magazine* 6, no. 41 (1921): 295.

Uzzal, Rajib Alam, Rama B. Bhat, and Waiz Ahmed. "Dynamic response of a beam subjected to moving load and moving mass supported by Pasternak foundation." *Shock and Vibration* 19, no. 2 (2012): 205-220.

Weaver Jr, William, Stephen P. Timoshenko, and Donovan Harold Young. *Vibration problems in engineering*. John Wiley & Sons, 1990.

Appendixes

Appendix I Dimensionless Frequencies of Euler-Bernoulli Beams

```
% Input otational spring constants T1,T2 and vertical spring constants R1,R2
% K is dimensionless frequency

R1=10*E*I/L;R2=20*E*I/L;
T1=9999999;T2=9999999;


clc
clear
k=2/3;M=4;A=1;r=0.02;E=30000;e=0.28;L=14.4;G=3*E/8;
I=r*r*A*L*L;
s=0.04;
syms K
A1=R1;
A2=E*I*K/L;
A3=R1;
A4=-E*I*K/L;
B1=-E*I*K^3/L^3;
B2=T1;
B3=E*I*K^3/(L^3);
B4=T1;
C1=-E*I*K/L*sin(K)+R2*cos(K);
C2=-E*I*K/L*cos(K)-R2*sin(K);
C3=E*I*K/L*sinh(K)+R2*cosh(K)
C4=E*I*K/L*cosh(K)+R2*sinh(K);
D1=-E*I*K^3*cos(K)/(L^3)-T2*sin(K);
D2=E*I*K^3*sin(K)/(L^3)-T2*cos(K);
D3=E*I*K^3*cosh(K)/(L^3)-T2*sinh(K);
D4=E*I*K^3*sinh(K)/(L^3)-T2*cosh(K);
H=[A1,A2,A3,A4;B1,B2,B3,B4;C1,C2,C3,C4;D1,D2,D3,D4];
Det=det(H)
f1=inline(Det,'K')
z=zeros(21,1);
for y= 1:1:20
K=fsolve(f1,y)
z(y+1)=K;
end
fid=fopen('N1.txt','wt');
%4.3f\n is the statistical form of the array
fprintf(fid,'%4.4f\n',z)
```

Appendix II Dimensionless Frequencies of Timoshenko Beams

```
% Input rotational spring constants T1,T2 and vertical spring constants R1,R2
% x is dimensionless frequency

T1=999999999;T2=999999999;R1=10*E*I/L;R2=20*E*I/L;

k=2/3;M=4;A=1;r=0.02;E=30*10^6;e=0.28/(32.2/12);L=14.4;G=3*E/8;
I=r*r*A*L*L;
s=0.04;

syms x
a=1/sqrt(2)*sqrt(-(r^2+s^2)+sqrt((r^2-s^2)^2+4/x^4));
b=1/sqrt(2)*sqrt((r^2+s^2)+sqrt((r^2-s^2)^2+4/x^4));
A1=-T1*L*(a)/(x^2*((a)^2+s^2));
A2=-E*A*s^2/(M*((a)^2+s^2));
A3=T1*L*b/(x^2*((b)^2-s^2));
A4=E*A*s^2/(M*((b)^2-s^2));
B1=E*I*x^2*(a)/L;
B2=-R1;
B3=E*I*x^2*(b)/L;
B4=-R1;
C1=(E*A*s^2*x^2*sinh(x^2*a)/M-T2*L*a*cosh(x^2*a))/(x^2*((a)^2+s^2));
C2=(E*A*s^2*x^2*cosh(x^2*a)/M-T2*L*a*sinh(x^2*a))/(x^2*((a)^2+s^2));
C3=(-E*A*s^2*x^2*sin(x^2*b)/M+T2*L*b*cos(x^2*b))/(x^2*((b)^2-s^2));
C4=(-E*A*s^2*x^2*cos(x^2*b)/M-T2*L*b*sin(x^2*b))/(x^2*((b)^2-s^2));
D1=(E*I*x^2*a*cosh(x^2*a)+R2*L*sinh(x^2*a))/L;
D2=(E*I*x^2*a*sinh(x^2*a)+R2*L*cosh(x^2*a))/L;
D3=(E*I*x^2*b*cos(x^2*b)+R2*L*sin(x^2*b))/L;
D4=(-E*I*x^2*b*sin(x^2*b)+R2*L*cos(x^2*b))/L;
H=[A1,A2,A3,A4;B1,B2,B3,B4;C1,C2,C3,C4;D1,D2,D3,D4];
Det=det(H)
f1=inline(Det,'x')
z=zeros(21,1);
for y= 1:1:20
x=fsolve(f1,y)
z(y+1)=x;
end
fid=fopen('N1.txt','wt');
%4.3f\n is the statistical form of the array
fprintf(fid,'%4.4f\n',z)
```

Appendix III First Five Mode shapes for Euler-Bernoulli Beams

```
% Input the first five frequencies K
% Input rotational spring constants T1,T2 and vertical spring constants R1,R2

%% Mode 1
K=2.1515;
k=2/3;M=4;A=1;r=0.02;E=30000;e=0.28;L=14.4;G=3*E/8;
I=r*r*A*L*L;
s=0.04;
R1=10*E*I/L;R2=20*E*I/L;
T1=9999999;T2=9999999;

A1=R1;
A2=E*I*K/L;
A3=R1;
A4=-E*I*K/L;
B1=-E*I*K^3/L^3;
B2=T1;
B3=E*I*K^3/(L^3);
B4=T1;
C1=-E*I*K/L*sin(K)+R2*cos(K);
C2=-E*I*K/L*cos(K)-R2*sin(K);
C3=E*I*K/L*sinh(K)+R2*cosh(K)
C4=E*I*K/L*cosh(K)+R2*sinh(K);
D1=-E*I*K^3*cos(K)/(L^3)-T2*sin(K);
D2=E*I*K^3*sin(K)/(L^3)-T2*cos(K);
D3=E*I*K^3*cosh(K)/(L^3)-T2*sinh(K);
D4=E*I*K^3*sinh(K)/(L^3)-T2*cosh(K);
H=[A1,A2,A3,A4;B1,B2,B3,B4;C1,C2,C3,C4;D1,D2,D3,D4];
E11=[A1,A2,A3;B1,B2,B3;C1,C2,C3];E10=[A4;B4;C4];E01=[D1,D2,D3];E00=[D4];
MM=-inv(E11)*E10;
E1=MM(1);E2=MM(2);E3=MM(3);E4=1;
t=0:0.001:1;
U12=E1*sin(K*t)+E2*cos(K*t)+E3*sinh(K*t)+cosh(K*t)
hold on
plot(t,U12,':b');

%% Mode 2
K=5.0605;
k=2/3;M=4;A=1;r=0.02;E=30000;e=0.28;L=14.4;G=3*E/8;
I=r*r*A*L*L;
s=0.04;
R1=10*E*I/L;R2=20*E*I/L;
T1=9999999;T2=0;

A1=R1;
A2=E*I*K/L;
A3=R1;
A4=-E*I*K/L;
B1=-E*I*K^3/L^3;
B2=T1;
B3=E*I*K^3/(L^3);
B4=T1;
```

```
C1=-E*I*K/L*sin(K)+R2*cos(K);
C2=-E*I*K/L*cos(K)-R2*sin(K);
C3=E*I*K/L*sinh(K)+R2*cosh(K)
C4=E*I*K/L*cosh(K)+R2*sinh(K);
D1=-E*I*K^3*cos(K)/(L^3)-T2*sin(K);
D2=E*I*K^3*sin(K)/(L^3)-T2*cos(K);
D3=E*I*K^3*cosh(K)/(L^3)-T2*sinh(K);
D4=E*I*K^3*sinh(K)/(L^3)-T2*cosh(K);
H=[A1,A2,A3,A4;B1,B2,B3,B4;C1,C2,C3,C4;D1,D2,D3,D4];
E11=[A1,A2,A3;B1,B2,B3;C1,C2,C3];E10=[A4;B4;C4];E01=[D1,D2,D3];E00=[D4];
MM=-inv(E11)*E10;
E1=MM(1);E2=MM(2);E3=MM(3);E4=1;
t=0:0.001:1;
U22=E1*sin(K*t)+E2*cos(K*t)+E3*sinh(K*t)+cosh(K*t)
hold on
plot(t,U22,':b');

%% mode 3
K=8.0538;
k=2/3;M=4;A=1;r=0.02;E=30000;e=0.28;L=14.4;G=3*E/8;
I=r*r*A*L*L;
s=0.04;
R1=10*E*I/L;R2=20*E*I/L;
T1=9999999;T2=0;

A1=R1;
A2=E*I*K/L;
A3=R1;
A4=-E*I*K/L;
B1=-E*I*K^3/L^3;
B2=T1;
B3=E*I*K^3/(L^3);
B4=T1;
C1=-E*I*K/L*sin(K)+R2*cos(K);
C2=-E*I*K/L*cos(K)-R2*sin(K);
C3=E*I*K/L*sinh(K)+R2*cosh(K)
C4=E*I*K/L*cosh(K)+R2*sinh(K);
D1=-E*I*K^3*cos(K)/(L^3)-T2*sin(K);
D2=E*I*K^3*sin(K)/(L^3)-T2*cos(K);
D3=E*I*K^3*cosh(K)/(L^3)-T2*sinh(K);
D4=E*I*K^3*sinh(K)/(L^3)-T2*cosh(K);
H=[A1,A2,A3,A4;B1,B2,B3,B4;C1,C2,C3,C4;D1,D2,D3,D4];
E11=[A1,A2,A3;B1,B2,B3;C1,C2,C3];E10=[A4;B4;C4];E01=[D1,D2,D3];E00=[D4];
MM=-inv(E11)*E10;
E1=MM(1);E2=MM(2);E3=MM(3);E4=1;
t=0:0.001:1;
U32=E1*sin(K*t)+E2*cos(K*t)+E3*sinh(K*t)+cosh(K*t)
hold on
plot(t,U32,':b');



%mode 4
K=11.0832;
```

```
k=2/3;M=4;A=1;r=0.02;E=30000;e=0.28;L=14.4;G=3*E/8;
I=r*r*A*L*L;
s=0.04;
R1=10*E*I/L;R2=20*E*I/L;
T1=9999999;T2=0;

R1=9999999; R2=0;T1=9999999;T2=0;
A1=R1;
A2=E*I*K/L;
A3=R1;
A4=-E*I*K/L;
B1=-E*I*K^3/L^3;
B2=T1;
B3=E*I*K^3/(L^3);
B4=T1;
C1=-E*I*K/L*sin(K)+R2*cos(K);
C2=-E*I*K/L*cos(K)-R2*sin(K);
C3=E*I*K/L*sinh(K)+R2*cosh(K)
C4=E*I*K/L*cosh(K)+R2*sinh(K);
D1=-E*I*K^3*cos(K)/(L^3)-T2*sin(K);
D2=E*I*K^3*sin(K)/(L^3)-T2*cos(K);
D3=E*I*K^3*cosh(K)/(L^3)-T2*sinh(K);
D4=E*I*K^3*sinh(K)/(L^3)-T2*cosh(K);
H=[A1,A2,A3,A4;B1,B2,B3,B4;C1,C2,C3,C4;D1,D2,D3,D4];
E11=[A1,A2,A3;B1,B2,B3;C1,C2,C3];E10=[A4;B4;C4];E01=[D1,D2,D3];E00=[D4];
MM=-inv(E11)*E10;
E1=MM(1);E2=MM(2);E3=MM(3);E4=1;
t=0:0.001:1;
U42=E1*sin(K*t)+E2*cos(K*t)+E3*sinh(K*t)+cosh(K*t)
hold on
plot(t,U42,':b');
xlabel('Normalized length')
ylabel('Amplitude')




%mode 5
K=14.1371;
k=2/3;M=4;A=1;r=0.02;E=30000;e=0.28;L=14.4;G=3*E/8;
I=r*r*A*L*L;
s=0.04;
R1=10*E*I/L;R2=20*E*I/L;
T1=9999999;T2=0;

A1=R1;
A2=E*I*K/L;
A3=R1;
A4=-E*I*K/L;
B1=-E*I*K^3/L^3;
B2=T1;
B3=E*I*K^3/(L^3);
B4=T1;
C1=-E*I*K/L*sin(K)+R2*cos(K);
C2=-E*I*K/L*cos(K)-R2*sin(K);
```

```
C3=E*I*K/L*sinh(K)+R2*cosh(K)
C4=E*I*K/L*cosh(K)+R2*sinh(K);
D1=-E*I*K^3*cos(K)/(L^3)-T2*sin(K);
D2=E*I*K^3*sin(K)/(L^3)-T2*cos(K);
D3=E*I*K^3*cosh(K)/(L^3)-T2*sinh(K);
D4=E*I*K^3*sinh(K)/(L^3)-T2*cosh(K);
H=[A1,A2,A3,A4;B1,B2,B3,B4;C1,C2,C3,C4;D1,D2,D3,D4];
E11=[A1,A2,A3;B1,B2,B3;C1,C2,C3];E10=[A4;B4;C4];E01=[D1,D2,D3];E00=[D4];
MM=-inv(E11)*E10;
E1=MM(1);E2=MM(2);E3=MM(3);E4=1;
t=0:0.001:1;
U52=E1*sin(K*t)+E2*cos(K*t)+E3*sinh(K*t)+cosh(K*t)
hold on
plot(t,U52,':b');



% super imposed mode shape
U62=(U12+U22+U32+U42+U52);
plot(t,U62,':r')
hold off
```

Appendix IV First Five Mode shapes for Timoshenko Beams

```
% Input the first five frequencies x
% Input rotational spring constants T1,T2 and vertical spring constants R1,R2


% Mode 1
x=1.8708;
k=2/3;M=4;A=1;r=0.02;E=30000;e=0.28;L=14.4;
I=r*r*A*L*L;
s=0.04;
a=1/sqrt(2)*sqrt(-(r^2+s^2)+sqrt((r^2-s^2)^2+4/x^4));
b=1/sqrt(2)*sqrt((r^2+s^2)+sqrt((r^2-s^2)^2+4/x^4));
A1=-T1*L*(a)/(x^2*((a)^2+s^2));
A2=-E*A*s^2/(M*((a)^2+s^2));
A3=T1*L*b/(x^2*((b)^2-s^2));
A4=E*A*s^2/(M*((b)^2-s^2));
B1=E*I*x^2*(a)/L;
B2=-R1;
B3=E*I*x^2*(b)/L;
B4=-R1;
C1=(E*A*s^2*x^2*sinh(x^2*a)/M-T2*L*a*cosh(x^2*a))/(x^2*((a)^2+s^2));
C2=(E*A*s^2*x^2*cosh(x^2*a)/M-T2*L*a*sinh(x^2*a))/(x^2*((a)^2+s^2));
C3=(-E*A*s^2*x^2*sin(x^2*b)/M+T2*L*b*cos(x^2*b))/(x^2*((b)^2-s^2));
C4=(-E*A*s^2*x^2*cos(x^2*b)/M-T2*L*b*sin(x^2*b))/(x^2*((b)^2-s^2));
D1=(E*I*x^2*a*cosh(x^2*a)+R2*L*sinh(x^2*a))/L;
D2=(E*I*x^2*a*sinh(x^2*a)+R2*L*cosh(x^2*a))/L;
D3=(E*I*x^2*b*cos(x^2*b)+R2*L*sin(x^2*b))/L;
D4=(-E*I*x^2*b*sin(x^2*b)+R2*L*cos(x^2*b))/L;
H=[A1,A2,A3,A4;B1,B2,B3,B4;C1,C2,C3,C4;D1,D2,D3,D4];
E11=[A1,A2,A3;B1,B2,B3;C1,C2,C3];E10=[A4;B4;C4];E01=[D1,D2,D3];E00=[D4];
MM=-inv(E11)*E10;
E1=MM(1);E2=MM(2);E3=MM(3);E4=1;
t=0:0.001:1;
p=x^2
S1=(E1*L*a*cosh(p*a*t)/(p*(a^2+s^2))+E2*L*a*sinh(p*a*t)/(p*(a^2+s^2))-
E3*L*b*cos(p*b*t)/(p*(b^2-s^2))+E4*L*b*sin(p*b*t)/(p*(b^2-s^2)));
Y1=(((p*(a^2+s^2))/(E1*L*a)))*S1;
hold on
plot(t,Y1,':b');
xlabel('Normalized length')
ylabel('Amplitude')

% Mode 2
x=4.621109;
k=2/3;M=4;A=1;r=0.02;E=30000;e=0.28;L=14.4;
I=r*r*A*L*L;
s=0.04;
a=1/sqrt(2)*sqrt(-(r^2+s^2)+sqrt((r^2-s^2)^2+4/x^4));
b=1/sqrt(2)*sqrt((r^2+s^2)+sqrt((r^2-s^2)^2+4/x^4));
A1=-T1*L*(a)/(x^2*((a)^2+s^2));
A2=-E*A*s^2/(M*((a)^2+s^2));
A3=T1*L*b/(x^2*((b)^2-s^2));
A4=E*A*s^2/(M*((b)^2-s^2));
```

```
B1=E*I*x^2*(a)/L;
B2=-R1;
B3=E*I*x^2*(b)/L;
B4=-R1;
C1=(E*A*s^2*x^2*sinh(x^2*a)/M-T2*L*a*cosh(x^2*a))/(x^2*((a)^2+s^2));
C2=(E*A*s^2*x^2*cosh(x^2*a)/M-T2*L*a*sinh(x^2*a))/(x^2*((a)^2+s^2));
C3=(-E*A*s^2*x^2*sin(x^2*b)/M+T2*L*b*cos(x^2*b))/(x^2*((b)^2-s^2));
C4=(-E*A*s^2*x^2*cos(x^2*b)/M-T2*L*b*sin(x^2*b))/(x^2*((b)^2-s^2));
D1=(E*I*x^2*a*cosh(x^2*a)+R2*L*sinh(x^2*a))/L;
D2=(E*I*x^2*a*sinh(x^2*a)+R2*L*cosh(x^2*a))/L;
D3=(E*I*x^2*b*cos(x^2*b)+R2*L*sin(x^2*b))/L;
D4=(-E*I*x^2*b*sin(x^2*b)+R2*L*cos(x^2*b))/L;
H=[A1,A2,A3,A4;B1,B2,B3,B4;C1,C2,C3,C4;D1,D2,D3,D4];
E11=[A1,A2,A3;B1,B2,B3;C1,C2,C3];E10=[A4;B4;C4];E01=[D1,D2,D3];E00=[D4];
MM=-inv(E11)*E10;
E1=MM(1);E2=MM(2);E3=MM(3);E4=1;
t=0:0.001:1;
p=x^2
S2=(E1*L*a*cosh(p*a*t)/(p*(a^2+s^2))+E2*L*a*sinh(p*a*t)/(p*(a^2+s^2))-
E3*L*b*cos(p*b*t)/(p*(b^2-s^2))+E4*L*b*sin(p*b*t)/(p*(b^2-s^2)));
Y2=((p*(a^2+s^2))/(E1*L*a))*S2
plot(t,Y2,':b')

% Mode 3
x=7.5809;
k=2/3;M=4;A=1;r=0.02;E=30000;e=0.28;L=14.4;
I=r*r*A*L*L;
s=0.04;
a=1/sqrt(2)*sqrt(-(r^2+s^2)+sqrt((r^2-s^2)^2+4/x^4));
b=1/sqrt(2)*sqrt((r^2+s^2)+sqrt((r^2-s^2)^2+4/x^4));
A1=-T1*L*(a)/(x^2*((a)^2+s^2));
A2=-E*A*s^2/(M*((a)^2+s^2));
A3=T1*L*b/(x^2*((b)^2-s^2));
A4=E*A*s^2/(M*((b)^2-s^2));
B1=E*I*x^2*(a)/L;
B2=-R1;
B3=E*I*x^2*(b)/L;
B4=-R1;
C1=(E*A*s^2*x^2*sinh(x^2*a)/M-T2*L*a*cosh(x^2*a))/(x^2*((a)^2+s^2));
C2=(E*A*s^2*x^2*cosh(x^2*a)/M-T2*L*a*sinh(x^2*a))/(x^2*((a)^2+s^2));
C3=(-E*A*s^2*x^2*sin(x^2*b)/M+T2*L*b*cos(x^2*b))/(x^2*((b)^2-s^2));
C4=(-E*A*s^2*x^2*cos(x^2*b)/M-T2*L*b*sin(x^2*b))/(x^2*((b)^2-s^2));
D1=(E*I*x^2*a*cosh(x^2*a)+R2*L*sinh(x^2*a))/L;
D2=(E*I*x^2*a*sinh(x^2*a)+R2*L*cosh(x^2*a))/L;
D3=(E*I*x^2*b*cos(x^2*b)+R2*L*sin(x^2*b))/L;
D4=(-E*I*x^2*b*sin(x^2*b)+R2*L*cos(x^2*b))/L;
H=[A1,A2,A3,A4;B1,B2,B3,B4;C1,C2,C3,C4;D1,D2,D3,D4];
E11=[A1,A2,A3;B1,B2,B3;C1,C2,C3];E10=[A4;B4;C4];E01=[D1,D2,D3];E00=[D4];
MM=-inv(E11)*E10;
E1=MM(1);E2=MM(2);E3=MM(3);E4=1;
t=0:0.001:1;
p=x^2
S3=(E1*L*a*cosh(p*a*t)/(p*(a^2+s^2))+E2*L*a*sinh(p*a*t)/(p*(a^2+s^2))-
E3*L*b*cos(p*b*t)/(p*(b^2-s^2))+E4*L*b*sin(p*b*t)/(p*(b^2-s^2)));
Y3=(((p*(a^2+s^2))/(E1*L*a)))*S3;
plot(t,Y3,':b')
```

```
% Mode 4
x=10.340520;
k=2/3;M=4;A=1;r=0.02;E=30000;e=0.28;L=14.4;
I=r*r*A*L*L;
s=0.04;
a=1/sqrt(2)*sqrt(-(r^2+s^2)+sqrt((r^2-s^2)^2+4/x^4));
b=1/sqrt(2)*sqrt((r^2+s^2)+sqrt((r^2-s^2)^2+4/x^4));
A1=-T1*L*(a)/(x^2*((a)^2+s^2));
A2=-E*A*s^2/(M*((a)^2+s^2));
A3=T1*L*b/(x^2*((b)^2-s^2));
A4=E*A*s^2/(M*((b)^2-s^2));
B1=E*I*x^2*(a)/L;
B2=-R1;
B3=E*I*x^2*(b)/L;
B4=-R1;
C1=(E*A*s^2*x^2*sinh(x^2*a)/M-T2*L*a*cosh(x^2*a))/(x^2*((a)^2+s^2));
C2=(E*A*s^2*x^2*cosh(x^2*a)/M-T2*L*a*sinh(x^2*a))/(x^2*((a)^2+s^2));
C3=(-E*A*s^2*x^2*sin(x^2*b)/M+T2*L*b*cos(x^2*b))/(x^2*((b)^2-s^2));
C4=(-E*A*s^2*x^2*cos(x^2*b)/M-T2*L*b*sin(x^2*b))/(x^2*((b)^2-s^2));
D1=(E*I*x^2*a*cosh(x^2*a)+R2*L*sinh(x^2*a))/L;
D2=(E*I*x^2*a*sinh(x^2*a)+R2*L*cosh(x^2*a))/L;
D3=(E*I*x^2*b*cos(x^2*b)+R2*L*sin(x^2*b))/L;
D4=(-E*I*x^2*b*sin(x^2*b)+R2*L*cos(x^2*b))/L;
H=[A1,A2,A3,A4;B1,B2,B3,B4;C1,C2,C3,C4;D1,D2,D3,D4];
E11=[A1,A2,A3;B1,B2,B3;C1,C2,C3];E10=[A4;B4;C4];E01=[D1,D2,D3];E00=[D4];
MM=-inv(E11)*E10;
E1=MM(1);E2=MM(2);E3=MM(3);E4=1;
t=0:0.001:1;
p=x^2
S4=(E1*L*a*cosh(p*a*t)/(p*(a^2+s^2))+E2*L*a*sinh(p*a*t)/(p*(a^2+s^2))-
E3*L*b*cos(p*b*t)/(p*(b^2-s^2))+E4*L*b*sin(p*b*t)/(p*(b^2-s^2)));
Y4=(((p*(a^2+s^2))/(E1*L*a)))*S4;
plot(t,Y4,':b')

% Mode 5
x=12.909686;
k=2/3;M=4;A=1;r=0.02;E=30000;e=0.28;L=14.4;
I=r*r*A*L*L;
s=0.04;
a=1/sqrt(2)*sqrt(-(r^2+s^2)+sqrt((r^2-s^2)^2+4/x^4));
b=1/sqrt(2)*sqrt((r^2+s^2)+sqrt((r^2-s^2)^2+4/x^4));
A1=-T1*L*(a)/(x^2*((a)^2+s^2));
A2=-E*A*s^2/(M*((a)^2+s^2));
A3=T1*L*b/(x^2*((b)^2-s^2));
A4=E*A*s^2/(M*((b)^2-s^2));
B1=E*I*x^2*(a)/L;
B2=-R1;
B3=E*I*x^2*(b)/L;
B4=-R1;
C1=(E*A*s^2*x^2*sinh(x^2*a)/M-T2*L*a*cosh(x^2*a))/(x^2*((a)^2+s^2));
C2=(E*A*s^2*x^2*cosh(x^2*a)/M-T2*L*a*sinh(x^2*a))/(x^2*((a)^2+s^2));
C3=(-E*A*s^2*x^2*sin(x^2*b)/M+T2*L*b*cos(x^2*b))/(x^2*((b)^2-s^2));
C4=(-E*A*s^2*x^2*cos(x^2*b)/M-T2*L*b*sin(x^2*b))/(x^2*((b)^2-s^2));
D1=(E*I*x^2*a*cosh(x^2*a)+R2*L*sinh(x^2*a))/L;
D2=(E*I*x^2*a*sinh(x^2*a)+R2*L*cosh(x^2*a))/L;
```

```
D3=(E*I*x^2*b*cos(x^2*b)+R2*L*sin(x^2*b))/L;
D4=(-E*I*x^2*b*sin(x^2*b)+R2*L*cos(x^2*b))/L;
H=[A1,A2,A3,A4;B1,B2,B3,B4;C1,C2,C3,C4;D1,D2,D3,D4];

E11=[A1,A2,A3;B1,B2,B3;C1,C2,C3];E10=[A4;B4;C4];E01=[D1,D2,D3];E00=[D4];
MM=-inv(E11)*E10;
E1=MM(1);E2=MM(2);E3=MM(3);E4=1;
t=0:0.001:1;
p=x^2
S5=(E1*L*a*cosh(p*a*t)/(p*(a^2+s^2))+E2*L*a*sinh(p*a*t)/(p*(a^2+s^2))-
E3*L*b*cos(p*b*t)/(p*(b^2-s^2))+E4*L*b*sin(p*b*t)/(p*(b^2-s^2)));
Y5=(((p*(a^2+s^2))/(E1*L*a)))*S5;
plot(t,Y5,':b')

Y66=(Y1+Y2+Y3+Y4+Y5);
plot(t,Y66,'-b')
```

Vita

Ye Tao was born in Jiangsu, China, on January 9, 1990, the daughter of Shijun Tao and Hong Chen. After finishing high school in 2008, she entered West Virginia University at Morgantown, West Virginia. She received the degree of Bachelor of Science in Civil and Environmental Engineering in May 2013. She continued her graduate study from August 2013, under the advisement of Dr. Roger Chen. Currently she is working at Dura-stress Inc. as a Structural Engineer, located nearby Orlando, Florida.